Use of isothermal calorimetry for predicting the shelf life of biologics in formulation

By

Benjamin Clarkson

A dissertation submitted to Johns Hopkins University in conformity with the requirements for the degree of Doctor of Philosophy

Baltimore, Maryland

February 2019

Abstract

Historically, drugs have mainly been small chemical compounds synthesized from natural sources. But with the advent of recombinant DNA technology, protein-based drugs, or biologics, have become a significant fraction of the pharmaceutical industry. Biologics are larger and more complex than standard small molecule drugs which gives them greater specificity and potency, but also makes them difficult to characterize and formulate. The primary issue is that at the high protein concentrations used in many formulations, biologics are prone to aggregation which can cause unsafe and painful drug administration. Common methods for characterization and analysis of protein stability and/or aggregation often require different physical or chemical conditions than those present in formulation and provide little or no predictive power, necessitating long incubation times for shelf life determination. To combat this problem and further our understanding of protein aggregation I have developed isothermal calorimetry for use in measuring the rates of unfolding and aggregation for high concentrations of protein at temperatures well below those used in traditional DSC experiments. I have compared and confirmed isothermal calorimetry results for a candidate HIV vaccine called VRC07-523LS in formulation to data obtained using other widely used experimental techniques and found that predictions of long-term stability rank order for a set of buffers correlate precisely with the results obtained using SEC. The ability to measure unfolding and aggregation rates at high protein concentrations and with relatively mild denaturing conditions results in more accurate predictions of the shelf life of biologics and allows the direct investigation of protein stability at the high concentrations used in formulations, improving our understanding of aggregation as a whole.

Thesis Committee Members:

Ernesto Freire (Thesis Advisor)

Bertrand Garcia-Moreno (Thesis Reader)

Christian Kaiser

Jamie Spangler

Acknowledgements

Completing my graduate degree would have been impossible without the guidance and support of so many people. Before graduate school, I don't think I had even heard the word "biophysics", had never taken a class in biochemistry, and would not have believed I'd get a degree incorporating aspects of both fields.

Any discussion of my journey from an undergraduate at Davidson to now would not be complete without thanking my undergraduate advisor and mentor, Malcolm Campbell. He provided me with my first intensive research experience, and his guidance and insightful advice were invaluable with propelling me to graduate school.

My graduate school experience owes much of its success to the members of my lab. I have learned so much about how to think about and present science from Ernesto, and his lectures on the basic principles of the underlying science are some of my most viewed reference materials. The ability to state complicated concepts in a simple and succinct line is one I continually hope to replicate. And Victoria has made so much of the daily rigors of lab work so easy, whether it's with an ear to complain to, or doing all of the thankless jobs that I prefer to avoid, from ordering all my supplies to cleaning DSCs when I'm feeling swamped. I don't know how other labs survive without someone like her to make sure everything is always running smoothly. Arne has provided so much support and been so giving in his vast scientific knowledge that I can't adequately thank him in just a few sentences. This thesis, among many other projects, would not have been possible without many fruitful discussions and kind words from him.

Finally, I would be remiss without thanking my family, who universally lack a scientific background, but never let that stop them from expressing their interest and support for my graduate work. Dad, thank you for sparking my interest in science at a young age with your daily observations on new and interesting companies you worked with, and continuing to keep me up to date on the latest and greatest of the biotech world. Mom, thank you for always being up for a talk when I was having writers block, and your excitement whenever I published a paper, even though you didn't understand it (Bev and Dick also get major points for that: I think Bev even took notes). Ethan, thank you for trying so hard to remember and understand what my research was about whenever I talked about it, the legal field will be lucky to have you as a part of it. And most of all, thank you from the bottom of my heart to Chelsea. I can't remember how many times you took my mind off a frustrating day and let me escape the stress of the graduate school grind. I am so lucky to be married to you.

Table of Contents

List of Figures and Tables

Intended to be blank

Chapter 1. Introduction

Biologics

For much of human history, medicines were limited to natural sources, mainly from various plants and fungi. In 1869 the first synthetic drug, chloral hydrate, was introduced as a sleeping aid (*4*). This marked the beginning of the age of "small molecule" drugs, often synthesized from the aforementioned natural sources, leading to the development of a fledgling pharmaceutical industry led by companies like Bayer in Germany (*4*). These companies largely grew out of the textile and synthetic dye industry and soon developed synthetic barbiturates, analgesics, and antipyretics, highlighted by the discovery of aspirin, which is still widely used and administered today (*4*). The serendipitous discovery of penicillin through observation of a contaminated Petri dish also provides an illustrative example of the drug development process during this time period. A major advance occurred in the 1970's with the development of recombinant DNA technology, which gave pharmaceutical companies more control over drug development through genetic engineering. Rather than identifying and mass producing naturally occurring drug molecules, now they could engineer microorganisms to produce lucrative and useful drugs. Genentech, a biotechnology company formed by University of California-San Francisco researchers in 1976, provided perhaps the best example of this new utility with the production of insulin using *Escherichia coli* in 1978 (*5*).

Today, the definition of biologics has grown with the ability to produce a wider array of molecules. Biologics are generally defined as any large molecule produced

from living cells used in the treatment or prevention of human disease (*6*). Rather than chemical synthesis, they are produced by genetically engineering animal cells, bacteria, or yeast to make the desired product. This engineering often adapts or exploits naturally occurring processes in the chosen cells, and the resulting products can be up to 1000 times larger than traditional small molecule drugs (*6*). Biologics now include a wide array of molecules, from monoclonal antibodies, to recombinant hormones, to targeted gene therapies, but the term is also often used to generally refer to any protein-based drug molecule (*7*).

With the expiration of patents on traditional chemical drugs, as well as the ability to specifically design biologics for particular targets, biologics are becoming one of the main sources of revenue for biotechnology and drug companies. Small molecules will likely always compose a significant fraction of available drugs, as they are less time consuming, easier, and cheaper to manufacture than biologics, as well as being orally bioavailable for ease of administration (*8*). But the advantages of biologics in regards to specificity and potency ensure that biologics will also maintain a significant market share. They have rapidly become, and are expected to continue to be, one of the largest segments of the pharmaceutical industry. Biologics are projected to make up 29% of the global pharmaceutical industry and 50 of the top 100 products by 2022 (*9*). More in-development biologics reaching the market as they gain approval will also contribute to this rapid increase in market share.

The greater size of biologics in comparison to small molecules also translates to significantly more complex molecular structures (*7*). The intricate secondary, tertiary, and even quaternary structures of biologics, plus post-translational modifications like

glycosylation, leads to much greater specificity but also poses a number of drawbacks. This complicated structure means that biologics are extremely sensitive to minute changes in manufacturing protocols which can significantly affect their medicinal and chemical properties (*7*). Their multi-step production methods are often subject to small amounts of variation that can affect the properties of the drug, and are also frequently around 100-fold more expensive than chemical production methods for small molecules (*7*). Further, characterizing their structural and physiochemical properties fully is often impossible, especially due to the fact that they can change with different manufacturing processes (*7*). Additional issues are caused by the almost universal immunogenicity of biologics. Drug companies seek to blunt the immune response in a variety of ways, frequently by using proteins that are partially or completely human homologs, but this is rarely a complete solution (*7*). It is also imperative that reducing immunogenicity begins at the molecular design level of development by minimizing antigenic epitopes and developing molecules with favorable physical and chemical properties (*7*). These immune responses may decrease the efficacy of the drug or lead to unwanted side effects, and can vary from low-level more generalized responses with very little consequences to the patient, to highly specific IgG responses that can potentially be life threatening (*7*). These immune responses are also notoriously difficult to predict through non-clinical studies using biochemical assays, and the complexity of the human immune system often necessitates immunogenicity analysis through human trials (*7*).

While oral administration is the gold standard for drug delivery, biologics are particularly difficult to take orally for a number of reasons. Chief among them is that biologics are rapidly degraded in the GI tract by acid and proteolytic enzymes.

Combined with their poor permeability, this leads to poor bioavailability when administered orally (*10*). In order to get around this problem, biologics are generally administered via intravenous (IV), subcutaneous (SC), or intramuscular (IM) injection. While IM injection is useful for between 2 and 5 mL injection volumes, it also is much more painful and has a high risk of complications due to the depth of the injection site below the skin (*11*). Generally speaking, biologics are formulated to be delivered through either IV or SC injections. IV administration is useful in that it can involve much higher volumes than other delivery methods and leads to rapid responses to the drug in the patient (*11*). The issue with IV injections is that they require trained medical personnel to administer, and are time consuming due to their often large volumes and the necessary observation of the patient after treatment for negative side effects (*11*). This occupies both valuable space in the treatment center, as well as the time of specialized personnel. SC administration is therefore the delivery method of choice for biologics in the absence of effective oral delivery. The primary advantages of SC injections are that they can be administered by the patient, are not particularly painful, and multiple injection sites can be used in the case of multiple dosing (*11*). This ease of administration leads to a higher rate of treatment compliance by patients as well as increasing their quality of life (*11*). The downside to SC injections is that they require volumes less than 1 or 2 mL, which then requires very high drug concentrations in the formulation in order to achieve proper dosage, on the order of 100 mg/mL or greater (*11*).

The high protein concentrations necessary for many biologic formulations can change the behavior of the proteins in solution and lead to a number of problems during

formulation development. The most common of these problems are increases in the viscosity of the solution, decreases in the stability of the protein, and increases in its aggregation (*12*). These issues can pose serious problems during drug development, transport, and storage, as well as eventual patient administration (*12*).

High viscosity makes using filtration methods to achieve high concentration formulations difficult by contributing to loss of sample in the filtering apparatus, as well as a higher back pressure on the filter itself (*13*). Injections of high viscosity solutions are also difficult and painful for patients to administer (*13*). This increase in viscosity with higher concentrations of protein is caused by weak intermolecular interactions between protein molecules (*14*). At higher protein concentrations there is a higher probability of individual protein molecules interacting than in dilute solutions, and this leads to the individually weak interactions between molecules having a larger overall effect on solution viscosity (*14*).

Although the viscosity of a formulation must be kept in mind during formulation development, it is almost exclusively dealt with at the earliest stage of drug molecule selection by choosing a molecule that exhibits low viscosity before different formulations are extensively tested. Once a specific drug molecule is chosen, it is often of greater concern and utility to monitor its stability and aggregation in a given formulation. Protein aggregation and its effect on stability will be discussed in depth in Chapter 2 of this work. In short, protein aggregation is a concentration dependent phenomenon, and, therefore, increases at higher protein concentrations. Aggregation shifts the equilibrium towards the aggregating species, thereby affecting the Gibbs free energy (ΔG), which describes the equilibrium of the system. ΔG increases with increasing concentration if

the protein aggregates in the native state, or decreases with increasing protein concentration if aggregation occurs in the denatured state.

Formulation development mainly involves identifying the formulation conditions in which the drug is most stable and easy to administer to patients. While ease of patient administration, with minimal pain at the site of administration, is a concern during development, the primary indicator of formulation performance is the long term stability of the drug molecule. Long term stability can be measured using a variety of methods, which will be discussed in more detail in the next section of this chapter. These methods generally measure the fraction of protein in different oligomeric states. As the active conformation of most drugs is native monomers, long term stability is usually quantitatively measured by the disappearance of monomer over time under different storage conditions.

A variety of factors are evaluated when choosing a formulation in order to insure relatively painless administration and drug stability, such as the pH and ionic strength of the buffer. But the primary tool used to improve the stability of a drug during formulation development once a general pH range is chosen for the formulation is the addition of excipients. Excipients are substances other than the drug or active ingredient that are added to the formulation. They can serve a variety of purposes, like adding bulk to a small amount of drug, enhancing drug absorption by the body, or protecting the protein from certain types of stress (*15*). Osmolytes, naturally ubiquitous small organic compounds that affect protein stability, are one of the largest classes of excipients (*16*). These compounds are classified as protecting or denaturing osmolytes based on whether they drive the equilibrium towards the native or unfolded state, respectively

(*16*). For formulation development, protecting osmolytes are most useful, as they help to maintain the drug in its active, folded conformation. They can be divided into three categories: (1) polyols, (2) some amino acids and (3) methylamines, each of which is thought to have evolved in response to different environmental stressors (*17*). Polyols, like glycerol, sucrose, and trehalose, are particularly adept at protecting against large temperature swings and moisture losses (*17*). Glycine, arginine, and some other amino acids are thought to have evolved to protect against extracellular environments with high salt concentrations (*17*). Methylamines, on the other hand, which include compounds like trimethylamine N-oxide (TMAO), can protect cells from the unwanted negative effects of urea-rich environments (*17*). But while these various classes of osmolytes may have evolved for different purposes in nature, they are all useful to varying degrees in protein formulations, particularly L-arginine and various polyols like sucrose and sorbitol.

When evaluating different formulations for a drug, as mentioned previously, the ideal formulation is one that minimizes protein aggregation and maintains the maximum fraction of protein in the active conformation in order to achieve maximum drug efficacy. A formulation that achieves these goals will also have maximal long-term stability, or shelf life. These terms refer to how long the fraction of protein in the active conformation remains above acceptable levels, which is of utmost importance when bringing a drug to market, as it will have to be transported and stored for months or even years before patient administration. This naturally leads to predicting and measuring the long term stability of drugs in different formulations as one of the most important aspects of formulation development. Numerous techniques can be used in

this respect, which will be discussed in the next section. Ones used to determine, rather than predict, the shelf life, typically measure the fraction of protein in different oligomeric states after different incubation times at various storage temperatures.

Techniques used to analyze biologics

Size exclusion chromatography (SEC) is one of the most widespread and useful techniques in the pharmaceutical industry for assessing the long-term aggregation of protein therapeutics. The technique itself is actually rather old, as size based separation of proteins was first theorized in 1944 and experimentally observed in 1955 (*18*). With the advent of protein-based therapeutics, it has seen a resurgence in interest and utility among pharmaceutical companies quantifying the aggregation of protein-based drugs.

SEC is performed by running buffer containing the protein of interest over a column packed with a porous matrix using a liquid chromatography system. This matrix, often referred to as the stationary phase, was originally composed of starch, but in the present day is composed of other materials (*18*). The packing material should ideally be totally non-reactive with proteins and be very mechanically stable (*18*). One of the most popular packing materials is cross-linked dextrans sold under the tradename Sephadex and originally developed by Pharmacia, but polyacrylamide based gels can also be used (*18*). When buffer is run through the stationary phase, particles are separated by size based on the amount of time they spend inside the porous spheres making up the packed column bed. Smaller particles are more likely to spend more time inside the spheres, while larger particles travel through the length of the

column with minimal occupancy inside the spheres, leading particles to elute from the column in size order from large to small as determined by their Stokes radius (*18*). Since the size of protein aggregates is directly proportional to the number of aggregated molecules, separating protein molecules by size is a simple and straightforward way of determining the degree of aggregation in a given sample. Changing the particle or pore size for the stationary phase can be used to optimize the column for specific molecular sizes.

The primary way that SEC is utilized in the formulation development pipeline is assessing the shelf life of drugs in different formulations. Samples are incubated at different storage temperatures for weeks at a time, and aliquots are taken out at numerous time points for aggregation assessment. In this manner, a time course of the amount of protein aggregation in a sample can easily be constructed for different formulations.

The draw backs to using SEC for aggregation assessment are mainly due to experimental constraints. The protein concentration for an SEC experiment needs to be rather low, much lower than the ~100 mg/mL protein concentrations in most formulations (*19*). The buffer used in the SEC run is also often not the same as the formulation buffer in order to minimize interactions between the stationary phase and the protein, which may be enhanced by certain excipients and can lead to results that do not reflect the true aggregation profile of the sample (*19*). This means that the aggregation of the protein in question is analyzed in a different chemical and physical environment than it is stored in, which may lead to inaccurate results or conclusions if aggregation is affected by this change in environment (*19*). If the molecules in question

are large enough, then they may even avoid entering the stationary phase particles altogether, and elute in the void volume of the column, thereby being indistinguishable from other particles in the void volume.

SEC is the preferred method for measuring protein aggregation during formulation development, but results can sometimes be misleading due to non-specific interactions between the column matrix and the drug of interest, thereby necessitating orthogonal methods to confirm the results. Analytical Ultracentrifugation (AUC) is responsible for much of our knowledge of macromolecules and their biophysical properties in solution gathered over much of the twentieth century (*19*). Starting around the 1970's, SEC began to replace AUC as the technique of choice for most researchers to assay protein aggregation and other structural parameters due to its ease of use (*19*). But with the realization that orthogonal techniques are often necessary to assess aggregation of biologics in solution, as well as a number of engineering and computational advances which have drastically improved the quality and quantity of information that can be obtained, AUC has seen a resurgence in use for analysis of biologics (*19*).

To conduct a standard sedimentation velocity AUC experiment, a sample is loaded in a sector shaped centerpiece. Depending on the instrument and experimental set up, a reference solution may or may not be necessary. The rotor is brought up to an appropriate speed and the concentration profile of the sample as a function of the radius at different times is collected and describes the migration pattern of all macromolecular species in the sample. These curves can then be fit to obtain sedimentation and diffusion coefficients for the sample, as well as to determine how many molecular

species are present in the sample (*19*). While performing the experiment itself is simple, the reason that AUC is likely better suited to a supporting role rather than replacing SEC altogether is due to the high cost of AUC instrumentation and the complexity of the data analysis. But while AUC may not overtake SEC in utility during the formulation development process, it can provide key insights and confirmation when odd or unexpected results are encountered using SEC or other more widely used techniques.

Light scattering measurements, particularly dynamic light scattering, are another very common way of assessing the aggregate content of a protein sample. Static (SLS) and dynamic (DLS) light scattering both have the same general set-up: a laser is focused on a clear cell containing dilute sample. While most of the light will pass through the sample, some portion will be scattered by the sample particles in solution, and the intensity of the scattered light is detected at one or more angles (usually 15°-180°) from the incident laser light. DLS differs from SLS in that the scattered light intensity (most commonly at a 90° angle) is monitored over millisecond timescales to monitor the diffusive properties of the particles in solution (*20*). There are numerous strategies to analyze the scattered light intensity in order to derive quantitative values describing the particles in question. Generally speaking, SLS experiments are used to determine sample parameters like molecular weight and particle size (*20*). DLS provides information on the hydrodynamic radius or radius of gyration, as well as the diffusion coefficient of the particles (*20*). Through various analyses, other quantities like the second virial coefficient can also be determined, which indicates whether solute-solvent interactions are attractive, repulsive, or neither (*20*). Together, especially in

conjunction with other techniques like SEC, light scattering is a useful tool to quickly determine the degree of aggregation present in a protein sample. MALLS (Multi-Angle Laser Light Scattering) is the primary type of light scattering used in conjunction with SEC, although it can also be used on its own. MALLS measures the time-averaged intensity of scattered light with detection at multiple different angles to report on the molar mass and size of particles in solution (*21*). It is often used online with SEC to collect qualitative information on the size-separated particles.

While light scattering, primarily DLS and MALLS, is a useful tool to use in conjunction with other methods like SEC, it has similar drawbacks. It requires much lower protein concentrations than those used in formulation, and also provides little predictive power. The interpretation of the various parameters obtained from a light scattering experiment like the second virial coefficient can also not be straightforward for certain situations and data analysis can be very complicated (*21*). Perhaps most importantly, light scattering is extremely sensitive to sample contamination such as dust particles, requiring filtration of the sample before measurements can be obtained, which can remove the aggregates of interest to the study (*21*). Light scattering is also purely a qualitative method with low resolution, so aggregates must be very large in comparison to monomers in order to be identified accurately (*21*).

Differential Scanning Calorimetry (DSC) is one of the work horse techniques of the drug development pipeline. It can quickly assess the temperature stability of a drug in different formulations and requires very little protein, but does come with some significant drawbacks. The technique measures the change in heat capacity of a protein in solution as the temperature is slowly increased from rather low (~10°C) where

the protein population is presumed to be almost completely folded, to a higher temperature (~100°C) where it is entirely unfolded. This unfolding transition is characterized by an endothermic heat capacity peak whose maximum value, at the midpoint of the unfolding transition, is referred to by the temperature at which it occurs (T_m, or melting temperature). The difference between the native and denatured state heat capacity baselines is called ΔC_p. This important quantity determines how drastically protein stability changes with temperature and is crucial for any sort of extrapolation of stability to room temperature or beyond (*22-25*). Using these parameters, a complete thermodynamic description of protein unfolding can be obtained, allowing the determination of ΔG at any temperature (*22-24*).

To thermodynamically analyze a DSC curve completely, an accurate determination of ΔC_p must be acquired, which can be difficult if the protein unfolds irreversibly. Reversibility is tested by scanning up to a temperature such that the protein is entirely unfolded, cooling it to near room temperature, and then rescanning the sample. If unfolding is reversible, the rescan after cooling will perfectly replicate the original scan. If the protein irreversibly unfolds, the rescan will, generally, be a flat line, as all of the protein is already unfolded. For biologics, this poses a problem, as larger proteins like antibodies tend to almost exclusively unfold irreversibly and precipitate out of solution, which is seen as a sharp exothermic drop in signal in DSCs equipped with a coin-shaped sample cell. While this still allows for a quick assessment of stability by the position of T_m, it makes a more detailed analysis of the curves difficult, if not impossible. Besides the inability to determine ΔC_p, the precipitation is so extreme that it can even affect the T_m, making the calculated values less reliable. In instruments equipped with a

capillary cell, the exothermic drop in signal is not observed (*25, 26*), and the full denaturation process can be observed and studied, although deconvoluting the curves into their respective kinetically controlled transitions characterized by both a calorimetric and activation enthalpy can be highly complex.

Isothermal Chemical Denaturation (ICD) refers to the denaturation of a protein with large concentrations of a chemical denaturant, most commonly urea or Guanidine Hydrochloride (GdnHCl). Monitoring the populations of folded and unfolded protein (usually through intrinsic fluorescence) at varying denaturant concentrations can be used to calculate ΔG values for protein in different formulations (*27, 28*). Conducting ICD experiments at increasing protein concentrations and comparing the calculated ΔG values can provide information on the aggregation propensity of a given protein-formulation pair, as well as what conformation the protein aggregates in(*29*). Since aggregation is a concentration dependent process, an increase in ΔG with increasing protein concentration indicates that the protein aggregates in the native state, while a decrease indicates denatured state aggregation, and no change points towards a lack of significant amounts of aggregation(*29*).

ICD has long been a useful technique for studying protein stability due to the empirical observation that there is a linear relationship between ΔG and protein concentration, making the determination of ΔG^o, the stability of the protein in no denaturant, a simple matter(*30, 31*). It can also be conducted at room temperature and doesn't require the specialized equipment of other techniques, as the only necessary instrumentation is a fluorometer to monitor the concentration of protein in various states through intrinsic tryptophan fluorescence.

But certain experimental factors limit the utility of ICD in formulation development. As with many of the techniques discussed in this work, it requires lower protein concentrations than those used in formulation. Also, since it requires molar concentrations of denaturant, it can be difficult to test formulations with high ionic strengths or high excipient concentrations, as solubility limits become an issue.

Proteins are in constant equilibrium between different conformations (e.g. native and denatured states) but the population of unfolded states at lower temperatures is generally small, especially for stable proteins used as drugs. This means that the rate of unfolding is very small, so much so that it can't be measured directly under storage conditions. But since unfolding is a kinetic process, the rate of unfolding increases with temperature, as can be seen in the sharp unfolding transitions of DSC thermograms. But in isothermal calorimetry, rather than scanning up in temperature as in DSC, the sample is held at an elevated temperature that is still well below the T_m. This elevated temperature raises the unfolding rate to a measureable level which can be measured using an isothermal calorimeter such as the Thermal Activity Monitor (TAM) from TA instruments or a conventional DSC used in isothermal scan mode. These calorimeters can precisely hold one temperature for long periods of time, allowing the measurement of very small amounts of heat absorbed and released from the sample. Plotting this "heat flow" as an evolution of time and fitting the data enables extraction of rate constants for the processes taking place in the sample that contribute to the heat flow.

IC is a promising technique for formulation development for numerous reasons. It can be conducted, and has a better signal-to-noise ratio, at formulation protein concentrations near 100 mg/mL as opposed to the lower concentrations used by other

techniques. This means that the aggregation of the protein in question is measured in precisely the same chemical and physical environment as it is stored in. IC also doesn't utilize the harsh denaturation conditions used in DSC or ICD, so the observed denaturation and aggregation may more accurately reflect the processes occurring during storage at low temperatures. IC also doesn't have any limitation as far as requiring reversible processes or certain structural elements like tryptophans in order to collect accurate data.

Antibody Structure

Antibodies (specifically IgG1 class) are one of the key molecules of the immune system, binding to pathogens and marking them for destruction by other immune cells. They have a characteristic "Y" shape composed of two antigen-binding (Fab) fragments and one crystallizable (Fc) fragment which come together at the "hinge" region (*2*). Each ~150 kDa antibody is symmetrical and is composed of two identical light-heavy chain pairs. Each Fab consists of a complete light chain and the VH and CH1 domains of the heavy chain, with the complementarity determining region (CDR) which determines antigen binding located at the tip of each Fab, involving both light and heavy chain regions (*2*). The Fc region, which dimerizes the light-heavy chain pairs, is composed of the CH2 and CH3 regions of the heavy

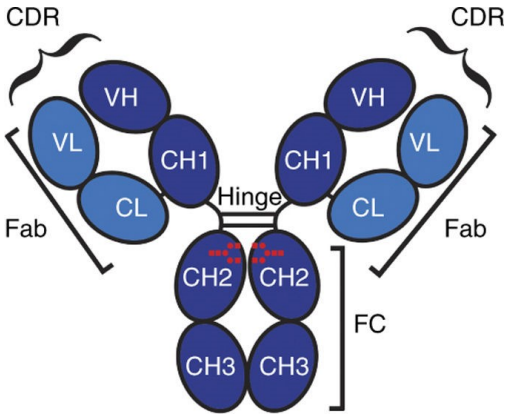

Figure 1-1. Structural features of an IgG monoclonal antibody. Domains making up the heavy chain (CH) are shown in dark blue, and light chain domains (CL) are shown in light blue (*2*).

chain (*2*). The heavy-light chain pairs are held together by disulfide bonds and are extensively glycosylated, particularly the CH2 domain, which further increases their complexity and can make production of homogeneous drug molecules difficult (*2*). These structural features are shown in **Figure 1-1**.

VRC07-523LS

Human Immunodeficiency Virus (HIV) is one of the great public health problems of modern times, but development of an effective vaccine has so far been unsuccessful. While treatment with antiretroviral and other drugs has dramatically increased the post-HIV infection lifetimes of patients, a vaccine that could prevent infection outright would be of great benefit. Therapeutic vaccines are a promising tool to prevent HIV-infection in high-risk individuals. The idea behind therapeutic vaccines is rather than convey immunity by "training" the immune system to recognize a particular pathogen, the body's immune system is boosted by an infusion of antibodies specific to the virus of interest to block infection. Treatment of at risk individuals with these anti-HIV antibodies during periods when the risk of transmission is high could prevent infection, such as treatment of a child to block mother-to-child transmission during birth.

VRC07-523LS is one such therapeutic vaccine in development at the Vaccine Research Center (VRC) and the National Institutes of Health. VRC07-523LS is a clonal relative of VRC01, one of the first therapeutic HIV vaccines developed at the VRC (*32*). VRC01 was isolated from the blood of a donor who was a slow HIV progressor, having maintained low HIV-1 RNA loads in serum without the use of antiretroviral drugs for over 18 years (*32*). It binds to the CD4 binding site of gp120 and blocks further infection (*32*). The VRC07 class of antibodies was identified through the sequencing of antibody-

gene transcripts for the same donor's B cells from whom VRC01 was isolated (*32*). The researchers made various targeted structural modifications to the originally isolated VRC07 to increase potency and decrease autoreactivity, eventually resulting in the optimized molecule VRC07-523LS, which will hereafter be referred to as VRC07 for simplicity (*32*).

Chapter 2. Protein Aggregation

Models of protein aggregation: Lumry-Eyring

Protein aggregation is problematic in most laboratory and industrial settings, and is therefore a subject of intense interest among researchers in a variety of fields. It is generally defined as the process by which originally monomeric protein self-assembles into high-molecular weight species, or aggregates, with non-native secondary structure (*33*). These aggregates are often high in β-sheet content, and their rate of formation is concentration dependent (*33*). Theoretically, a protein can aggregate in any of its adopted conformations. But by and large, the most common conformation from which aggregation proceeds is the denatured state, as unfolding exposes hydrophobic patches of the protein that can nucleate aggregation.

Irreversible denatured state aggregation is generally discussed using the simple scheme:

$$N \leftrightarrow U \rightarrow A$$

where *N* is the native state, *U* is the denatured state, and *A* is the aggregated state. This sort of two-step model, where the protein exists in equilibrium between two states, one of which can irreversibly aggregate, is known as the Lumry-Eyring model of

aggregation (*34*). In the case of native state aggregation, the irreversible conversion to *A* occurs from *N*. If the protein populates a partially denatured state, and this state undergoes irreversible aggregation, then the model involves two equilibria between *N* and *U* with the partially denatured state, plus one irreversible step from the partially denatured state. Applications of Lumry-Eyring models to different types of protein aggregation will be discussed in more detail in Chapter 4 of this manuscript, but will be briefly described here.

Thermodynamics of Protein Aggregation

Although proteins that undergo irreversible aggregation tend to do so from the denatured state, some proteins can undergo native state aggregation under certain conditions. Proteins that naturally form oligomers are a useful model to study this phenomena, such as the HIV-1 protease, which forms a dimer in the native state that dissociates upon unfolding (*35*). Since aggregation generally is thought to be caused by the exposing of hydrophobic groups upon partial or complete unfolding, native state aggregation is rare. Also, since the interactions that cause native state aggregation tend to be driven less by hydrophobicity, this aggregation tends to be at least partially reversible (*35*). Native state aggregation pushes the equilibrium to the left, towards the native state, increasing ΔG with protein concentration proportionally to the level of native association.

Since unfolding of a protein, even just a part of it, exposes hydrophobic groups which can nucleate aggregation, partially denatured or denatured state aggregation are the most common observed types. The main reason that more proteins that aggregate in the partially denatured state are not observed is likely due to the fact that stable

unfolding intermediates are rarer than simple two-state unfolding equilibria. For large, multi-domain proteins like monoclonal antibodies, however, aggregation of a partially denatured state is a significant concern. Aggregation in the partially denatured state pushes the equilibrium towards that state and away from the native and denatured states. This means that *ΔG* decreases with protein concentration for the $N \leftrightarrow P$ transition, where *P* is the partially denatured state, and *ΔG* increases with protein concentration for the $P \leftrightarrow U$ transition. If the partially denatured aggregate does not dissociate upon unfolding, then *ΔG* will only increase for the first transition while being independent of protein concentration for the second transition from partially denatured to fully denatured.

Fully denatured protein is generally the most prone to aggregation due to the large number of hydrophobic residues exposed upon unfolding. Aggregation in the denatured state drives the equilibrium towards the unfolded state, decreasing *ΔG* for the unfolding equilibrium with protein concentration.

The conformational stability of a protein clearly effects its aggregation propensity, particularly the stability of the native state. Since the native state is generally the least prone to aggregate of the available conformations, and a higher *ΔG* for the native-denatured state equilibrium means a higher fraction of protein in the native state, this leads to a decrease in the available states that can lead to aggregates. And since aggregates depopulate the native state, they have a direct effect on the conformational equilibrium. This means that excipients often utilize one of two different strategies to minimize aggregation: either stabilizing the native state, or the denatured state in order to prevent it from transitioning to an aggregated state. Increasing the stability of the

native state means that a greater fraction of protein is in the native state, and this conformation is less likely to aggregate than other conformations. The native state is also generally the active state for biologics, so maximizing the population of protein in the native state also leads to maximal potency for the drug. Stabilizing the denatured state can also prevent aggregation by increasing the fraction of protein in the denatured state instead of unwanted conformations. This is usually accomplished by the addition of excipients like L-Arginine which associate with the denatured state to solubilize it and prevent it from transitioning to an irreversibly aggregated state. While this approach successfully curtails aggregation, it also decreases ΔG for the first (unfolding) transition due to the association with the denatured state. This means that it is only effective if the stability of the protein without excipient is high enough that it can tolerate a slight decrease in stability in order to prevent aggregation.

Kinetics of Protein Aggregation

Since protein aggregation, particularly in the partially or fully denatured state, is an irreversible process, it is not governed by equilibrium thermodynamics. Instead, it is a kinetic process with rate constants that describe the speed with which a particular conformation becomes aggregated. These rate constants increase with temperature and, since aggregation is a concentration dependent phenomenon as discussed previously, they also increase with protein concentration. The simplest kinetic scheme for protein aggregation is a one-step irreversible reaction from some native state N to an aggregated state A:

$$N \xrightarrow{k} A$$

Where *k* is the rate constant describing the speed of the reaction. The disappearance of *N* over time can be described by a single-exponential (first-order) rate equation:

$$N = N_0 e^{-kt}$$

Where N_0 is the initial concentration of *N*. And since there are only two possible states for the protein, then the equation describing the concentration of *A* over time is simply:

$$A = N_0 - N_0 e^{-kt}$$

As any disappearance in *N* directly corresponds to an increase in *A*. Expressing the amounts of protein in each state in terms of fractions of the total population rather than individual concentrations further simplifies the above expressions, as assuming the population is entirely in the native state at the start of the reaction, N_0 can be replaced by 1.

But this one-step scheme is too simple to describe most aggregation reactions. A better model is one that is similar to the Lumry-Eyring model discussed previously for denatured state aggregation:

$$N \overset{k_u}{\rightarrow} U \overset{k_{agg}}{\longrightarrow} A$$

Where k_u is the overall rate of unfolding, and k_{agg} is the rate of irreversible aggregation from the unfolded state. The equations for this simplified model are similar to the one-step model above:

$$F_N = e^{-k_u t}$$

$$F_U = 1 - e^{-k_u t}$$

$$F_A = F_U(1 - e^{-k_{agg}t})$$

Where F_N, F_U, and F_A are the fraction of protein in the native, unfolded and aggregated states respectively. Since the rate of accumulation of protein in the aggregated state is dependent on both the rate of aggregation and the rate that protein unfolds, due to the fact that aggregation can only occur from the unfolded state, the behavior of the overall system depends on the relative magnitudes of the unfolding and aggregation rates. If the rates are similar, then unfolding and aggregation are well separated processes in

time, each described by their respective rate constants, as shown in **Figure 2-1A**. But if the aggregation rate is much faster than the unfolding rate, then the protein aggregates as soon as it unfolds and the overall process is described by a single rate constant, as shown in **Figure 2-1B**. The behavior becomes even more complex in an experimental context, such as in an isothermal calorimetry measurement. In such an experiment, the total heat associated with the unfolding and aggregation of the protein sample is proportional to the concentration of unfolded and aggregated protein and the heat associated with each process:

$$Heat = v\Delta H_u[U] + vQ_{agg}[Agg]$$

Where v is the sample volume, ΔH_u is the enthalpy of unfolding (endothermic), and Q_{agg} is the heat of irreversible aggregation (exothermic). The concentration of unfolded and aggregated protein can be rewritten in terms of the total protein concentration (P_T) and the fraction unfolded and fraction aggregated as:

$$Heat = v\Delta H_u[P_T]F_u + vQ_{agg}[P_T]F_uF_{agg}$$

The heat can then be normalized by the sample volume and the total protein concentration to express the heat only in

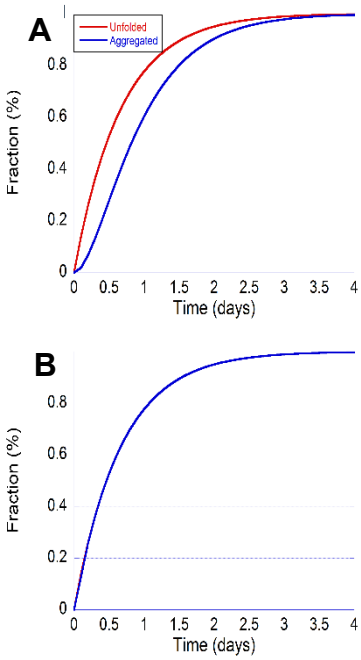

Figure 2-1. The relative magnitude of the rate constants effects the separation of unfolding and aggregation. **A)** The fraction unfolded and aggregated for a protein with equal unfolding and aggregation rates (1.5 $days^{-1}$). The processes are well separated, with aggregation lagging behind unfolding. **B)** When the aggregation rate is much faster than the unfolding rate, the fraction unfolded and fraction aggregated curves overlap and the overall process is described by a single rate constant.

terms of the fraction unfolded and fraction aggregated and the heats associated with each process:

$$Q = \frac{Heat}{v[P_T]} = \Delta H_u F_u + Q_{agg} F_u F_{agg}$$

F_u and F_{agg} can then be expressed in terms of the rate of unfolding and aggregation as discussed above:

$$Q = \Delta H_u(1 - e^{-k_u t}) + Q_{agg}(1 - e^{-k_u t})(1 - e^{-k_{agg} t})$$

Since the TAM actually measures the heat flow, or *dQ/dt* of a sample, we take the derivative of this above equation to get the equation used to model and fit isothermal calorimetry data:

$$\frac{dQ}{dt} = k_u \Delta H_u e^{-k_u t} + k_{agg} Q_{agg} e^{-k_{agg} t} + k_u Q_{agg} e^{-k_u t} - (k_u + k_{agg}) Q_{agg} e^{-(k_u + k_{agg})t}$$

Based on this equation, an isothermal calorimetry curve for a protein that unfolds and aggregates will be composed of an endothermic unfolding portion followed by an exothermic aggregation portion of the curve. The relative magnitudes of the rates and heats of unfolding and aggregation to each other will determine the final shape. In general, the heat of unfolding determines the magnitude of the endothermic portion of the curve while the rate of unfolding determines the steepness of that portion of the curve. On the other hand, the heat of aggregation determines the magnitude of the exothermic portion of the curve and the aggregation rate determines how broad that

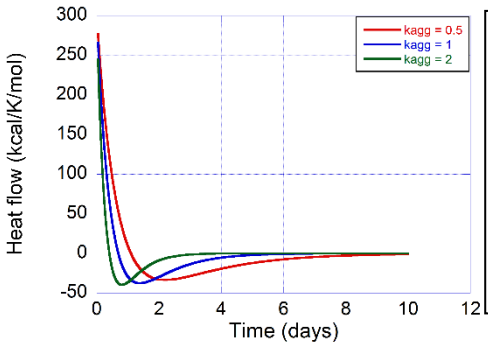

Figure 2-2. Simulated data in which ΔH_u and Q_{agg} are approximately equal. The location and width of the exothermic aggregation peak is determined by the magnitude of the two rate constants in proportion to each other. The value for k_u for each curve is 1 day^{-1}, while k_{agg} is varied between 0.5 and 2 days^{-1}.

portion of the curve is. Based on the relative magnitudes of the various parameters, a variety of curve shapes can be observed. If the unfolding enthalpy and aggregation heat are similar, then the ratio of the unfolding and aggregation rate constants determines the location and width of the exothermic aggregation portion of the curve, as shown in **Figure 2-2.**

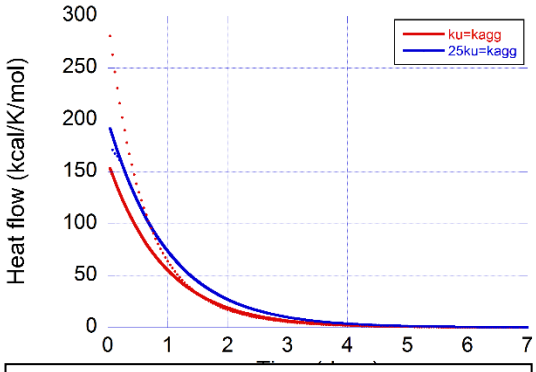

Figure 2-3. The relative magnitudes of the rate constants effects the shape of the heat flow curve. Simulated data for the case in which k_u = k_{agg} is shown in red with the associated single exponential fit as a solid line, and the case where k_{agg} = 25* k_u is shown in blue. The blue data is well described by a single exponential, while the red data is not.

If the aggregation rate is much higher than the unfolding rate, then the heat flow equation can be simplified to a single exponential:

$$\frac{dQ}{dt} = k_u(\Delta H_u + Q_{agg})e^{-k_u t} = k_u Q_{total} e^{-k_u t}$$

Where the total heat is a sum of the enthalpy of unfolding and the heat of aggregation. A curve with a k_{agg} 25 times greater than k_u is shown in comparison to a curve with equal unfolding and aggregation rates, along with single exponential fits, in **Figure 2-3**.

Chapter 3. Temperature Dependence of Rate Constants

Rate constants, much like equilibrium constants, are temperature dependent. While equilibrium constants can be described by the free energy of the equilibrium or its

associated enthalpy and entropy, rate constants can be described by the free energy of activation and the enthalpy and entropy of activation (indicated by a dagger superscript, †). The temperature dependence of rate constants can be described by:

$$\ln k = -\frac{\Delta G^{\dagger}}{RT} = -\frac{\Delta H^{\dagger} - T\Delta S^{\dagger}}{RT}$$

But the temperature dependence goes further, as it has been well established that both the enthalpy and entropy are temperature dependent due to the existence of a heat capacity difference between the native and denatured states. The temperature dependence of the activation enthalpy and entropy can be written as:

$$\Delta H^{\dagger} = \Delta H^{\dagger}_{ref} + \Delta C_p^{\dagger}(T - T_{ref})$$

$$\Delta S^{\dagger} = \Delta S^{\dagger}_{ref} + \Delta C_p^{\dagger} \ln(\frac{T}{T_{ref}})$$

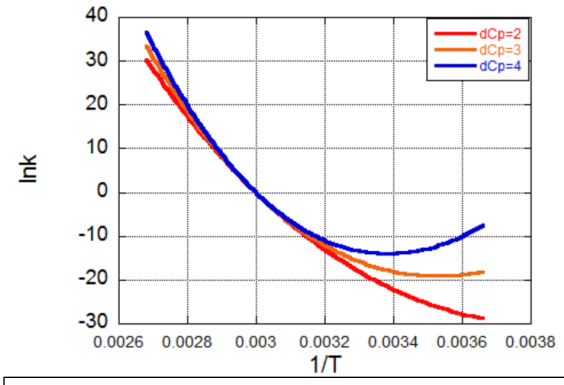

Figure 3-1. The magnitude of $\Delta C_p^{\dagger}$ affects the curvature of the rate constant temperature dependence curve, particularly at low temperatures. Arrhenius plot showing the natural log of the rate constant versus $1/T$ for simulated protein data in which all parameters are the same between curves except for $\Delta C_p^{\dagger}$ varying between 2 and 4 kcal/K/mol.

Using these equations, the effect of the different parameters on the rate constant over a wide temperature range can be observed. As can be readily seen from the equations, the existence of a $\Delta C_p^{\dagger}$ leads to non-linear Arrhenius plots, as shown in **Figure 3-1**. Examining the figure, it is readily apparent that while the rate constant is the same for all three curves at T_m, and the curves can be considered linear over short temperature stretches, especially at higher temperatures, the effect of a difference in $\Delta C_p^{\dagger}$ has a large effect on the rate constant at lower temperatures. This effect is crucial to consider when extrapolating rate constants to storage temperatures, since the effect of $\Delta C_p^{\dagger}$ is greater at lower temperatures. These lower temperatures are already very far away from T_m, which is generally the reference temperature that data is extrapolated from. Assuming linearity can lead to vast underestimations in the rate constant at storage temperatures due to this effect. An example of how much this $\Delta C_p^{\dagger}$ induced curvature can affect the value of the rate constant at lower storage temperatures is shown in the simulated data using typical parameters for globular proteins in **Figure 3-2**. While the blue protein has a T_m that is 20 degrees higher than the red, the 2 kcal/K/mol difference in their $\Delta C_p^{\dagger}$ leads to the red protein being more stable with a smaller rate constant at a storage temperature of 4°C by almost seven orders of magnitude. This clearly illustrates the large effect that small

changes in $\Delta C_p^{\ddagger}$ can have on the values of rate constants when extrapolating to low temperatures, as well as the pitfalls of assuming linearity over a wide range of temperatures in an Arrhenius plot, as $\Delta C_p^{\ddagger}$ causes pronounced curvature over wide temperature ranges. Since most measurements, even those presented in this work using isothermal calorimetry below T_m, are conducted well above the storage temperatures that data is extrapolated to, an understanding of $\Delta C_p^{\ddagger}$ is crucial for making accurate predictions. It is also crucial that any experimental determination of $\Delta C_p^{\ddagger}$ be extremely accurate, as small changes in its value can have very large effects on rate constants at low temperatures.

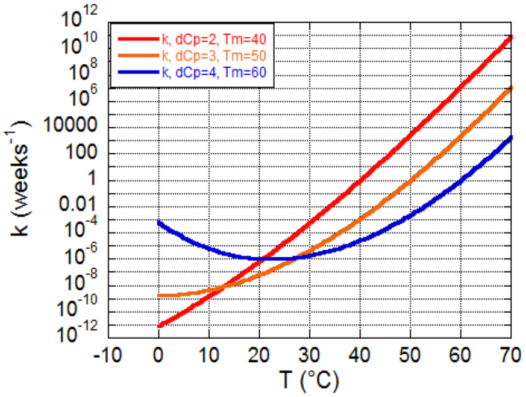

Figure 3-2. Small differences in $\Delta C_p^{\ddagger}$ can lead to large changes in the rate constant at low temperatures. Simulated data for three proteins with T_m values of 40, 50, and 60°C and $\Delta C_p^{\ddagger}$ values of 2, 3, and 4 kcal/K/mol for the red, orange, and blue curves respectively. The rate constant is shown versus T instead of lnk vs 1/T for clarity. All other parameters are the same for the three curves.

Chapter 4. Conformational stability and self-association equilibrium in biologics

This chapter was published in Drug Discovery Today (Clarkson et. al. 2015).

Introduction

The expected growth of biologics during the next years and their transformation from drugs administered mainly in hospital settings to drugs self-administered by

patients, requires the fulfilment of strict safety and stability conditions. The long term stability of biologics is a function of diverse physical and chemical factors that require different solutions. Among them, it becomes necessary to identify conditions that maximize the structural stability of the native state and prevent aggregation or other undesirable processes (*36*-*39*). Maximizing structural stability and minimizing aggregation tendencies involve decisions in at least two different development stages: the selection of the protein variants with the top stability/aggregation profiles; and, the identification of the solution conditions (formulations) that maximize stability and minimize aggregation. These decisions will be facilitated by a better understanding of the existing linkage between conformational and self-association processes.

Conformational Equilibrium in Proteins

Proteins exist in equilibrium between the native, partially denatured and fully denatured conformations. Even though there is an astronomical number of partially denatured (also referred to as partially folded) conformations, the vast majority never becomes populated. In fact, the native/denatured state equilibrium

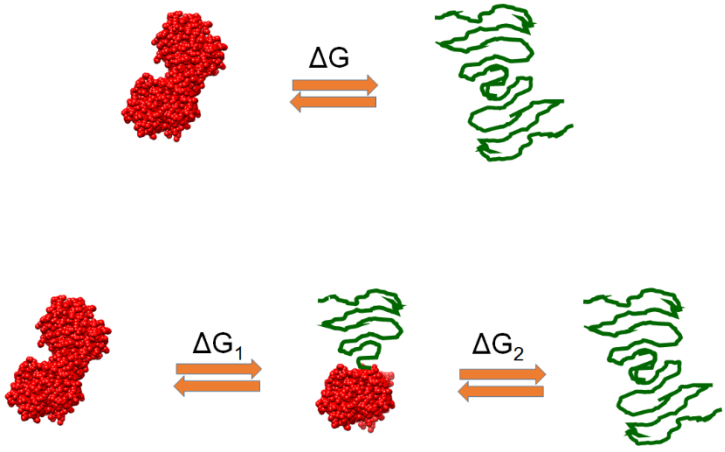

Figure 4-1. Typical protein denaturation situations encountered in the laboratory. The top panel illustrates the classical two-state situation in which protein denaturation occurs without the presence of partially denatured conformation. This situation is mostly observed for single domain proteins or multi-domain proteins with highly cooperative inter-domain interactions. The bottom panel illustrates the situation in which denaturation occurs with the presence of a significantly populated partially denatured state. This situation often occurs with multi-domain proteins.

of most single-domain proteins can be accounted for by the two-state model, in which the population of partially denatured conformations is negligible (*40*). Multi-domain proteins may exhibit partially denatured conformations corresponding to states in which some domains are unfolded while the others remain folded (*41*). **Figure 4-1** illustrates two commonly observed situations. The top panel represents the two-state situation in which the native and fully denatured conformations are the only ones that become significantly populated. The bottom panel represents the situation in which a partially denatured conformation becomes populated in addition to the native and fully denatured states. The partially denatured state usually originates from the unfolding of the least stable domain. In all cases, the stability of a protein or a structural domain is determined by the Gibbs energy of stability, ΔG,

Table 4-1

ΔG **kcal/mol**	**% Denatured Protein**
0	50
1.3	10
2.7	1
4.1	0.1
5.5	0.01
6.8	0.001
8.2	0.0001
9.6	0.00001
10.4	0.000001

characteristic of each structure. The population or fraction of denatured protein or domain is given by:

$$F_{denatured} = \frac{e^{-\frac{\Delta G}{RT}}}{1+e^{-\frac{\Delta G}{RT}}} \quad (4\text{-}1)$$

A large and positive ∆G minimizes the fraction of denatured protein. **Table 4-1** shows a look up table with characteristic ∆G values and the corresponding populations of denatured protein. The percent of denatured protein is simply the fraction denatured multiplied by 100. Also, the actual concentration of denatured protein is simply the total protein concentration multiplied by the fraction denatured. For example, in a 100mg/mL protein solution with a structural stability of 8 kcal/mol the concentration of denatured protein is 0.1µg/mL. In protein engineering or formulation development, a common goal is to optimize the structural stability of the protein, which is equivalent to maximizing ∆G. There are two techniques capable of measuring Gibbs energies and therefore able to provide a window into the conformational equilibrium of a protein: Differential Scanning Calorimetry (DSC) and Isothermal Chemical Denaturation (ICD). DSC induces protein denaturation by increasing the temperature of the solution (*24, 42, 43*), whereas ICD induces protein denaturation by the addition of a chemical denaturant, most commonly

urea or guanidine hydrochloride (*29-31, 44-46*). In both cases, the necessary requirement for ΔG determination is that the experimental measurement is performed under reversible conditions. This condition is tested by scanning the same sample twice or diluting the denatured concentration and recovering the original state.

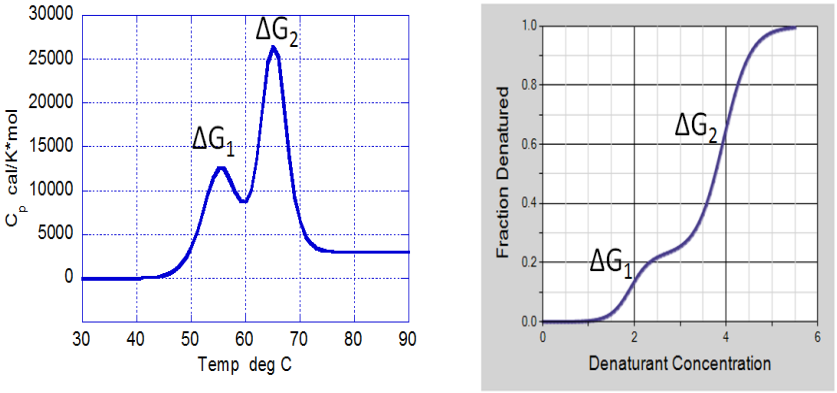

Figure 4-2. Differential scanning calorimetry (DSC) and isothermal chemical denaturation (ICD) allow measurement of the folding/unfolding reaction of a protein and determination of the Gibbs energy of stability (ΔG) for each step. Folding/unfolding thermodynamics can only be determined if the measurement is done under equilibrium conditions.

Figure 4-2 illustrates the type of data obtained by DSC and ICD for a protein characterized by the presence of two cooperative domains. In both cases, analysis of the data permits determination of ΔG_1 and ΔG_2 and their subsequent analysis (*24, 29-31, 42-46*).

Thermodynamic Linkage Between Conformational Equilibrium and Self-Association

Three immediate aggregation scenarios can be envisioned from the conformational equilibrium situations shown in **Figure 4-1**. The first case is the one in which the native state aggregates, the second case is the one in which the partially denatured state aggregates, and the third case the one in which the denatured state aggregates.

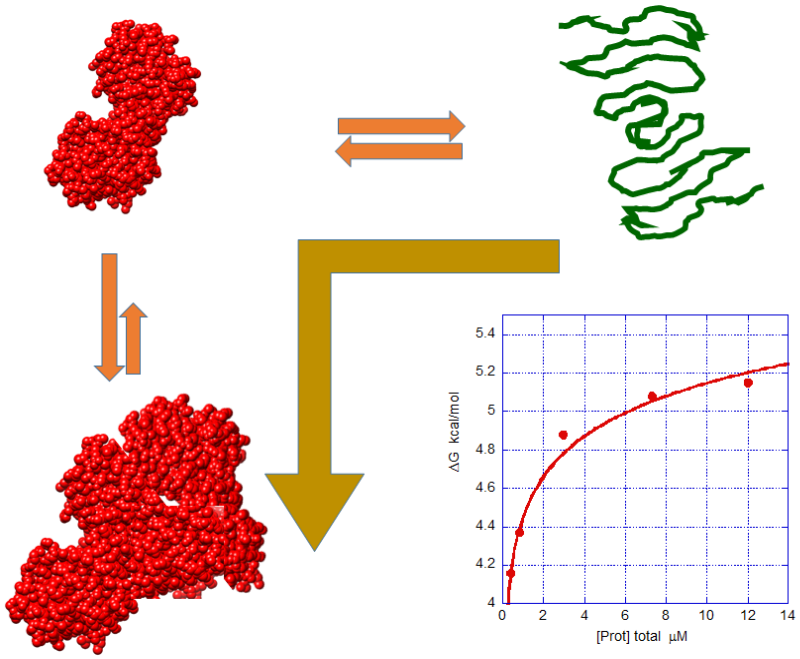

Figure 4-3. Self-association or aggregation of the native state is characterized by an increase in ΔG upon increasing protein concentration. The inset shows the example of the HIV-1 protease which is a dimer in the native state and dissociates upon unfolding. Denaturation experiments were performed using a linear gradient of guanidine hydrochloride from 0 to 5.5 M. The buffer was 10 mM sodium formate, pH 3.4. The final concentration of protease was varied from 0.4 to 12 uM. The exact concentration was determined from the absorbance at 280 nm using an extinction coefficient of 25,530 M^{-1} cm^{-1} (*3*). Gold arrows indicate direction of equilibrium shift.

Case 1: Native State Aggregation

Figure 4-3 illustrates the situation in which native state aggregation is present. In this case the equilibrium will be shifted to the left, ΔG of the denatured and partially denatured states will increase and, consequently, the stability of the native state will increase. If this situation occurs, the measured ΔG usually referred to as apparent ΔG is given by (*47*):

$$\Delta G_{app} = \Delta G_o^o + RTln(1 + jK_{N,j}[N]^{j-1}) \quad (4\text{-}2)$$

Where ΔG_o^o is equal to the value of the Gibbs energy extrapolated to zero protein concentration (in practice, a concentration low enough at which aggregation is not present). **Equation 4-2** indicates that native state aggregation will cause the measured Gibbs energy to increase as a function of protein concentration and that the magnitude of the increase is proportional to the aggregation constant and the average size of the aggregates. For the specific case in which the native state forms a dimer (j = 2), **equation 4-2** has an exact solution that can be expressed in terms of the total protein concentration as demonstrated before for the HIV-1 protease (*3*) (see inset in **Figure 4-3**). In this case, it is possible to determine the dimerization constant which under the conditions in the figure is 1.6 x 10^{-8} M. For arbitrary degrees of oligomerization, there are no exact solutions for $K_{N,j}$ but the fraction of aggregated protein can be calculated directly from the data even though j and $K_{N,j}$ cannot be determined:

$$F_{aggregated} = \frac{(e^{\frac{\Delta\Delta G}{RT}} - 1)}{(1 + e^{-\frac{\Delta G_O^O}{RT}} + \left(e^{\frac{\Delta\Delta G}{RT}} - 1\right))} \quad (4\text{-}3)$$

Where $\Delta\Delta G = \Delta G_{app} - \Delta G_o^o$. In general, if experiments are performed at different protein concentrations, an increase in the measured ΔG with protein concentration is indicative of native state aggregation or oligomerization.

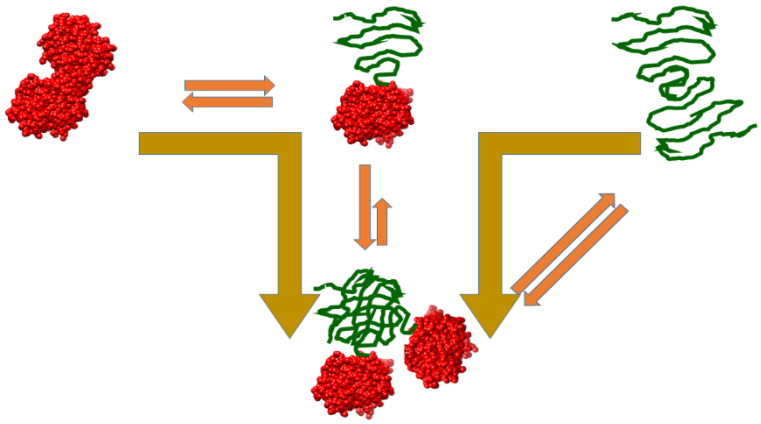

Figure 4-4. Partially denatured conformations might have a higher tendency to aggregate than the native or fully denatured state, in which case aggregation occurs when the partially denatured state becomes populated. In this case, dissociation occurs upon full denaturation. This behavior is exhibited by recombinant human growth hormone at low pH (*1*). Gold arrows indicate direction of equilibrium shift.

Case 2: Partially Denatured State Aggregation

In some situations, partially denatured conformations have a higher tendency to aggregate than the native or denatured states. The situation is illustrated in **Figure 4-4.** In this case, the first transition, corresponding to the transition from monomeric native to self-associated partially denatured states is shifted down upon increasing protein concentration whereas the second transition, corresponding to the transition from the self-associated partially denatured to monomeric fully denatured state is shifted up upon increasing protein concentration. Experimentally, this situation has been observed with recombinant human growth hormone (rHGH) at low pH (*1*). rHGH is a monomeric

protein, upon denaturation at low pH it forms a partially denatured dimer which fully dissociates upon complete denaturation. It must be noted that if the aggregated partially denatured state were the end point of the denaturation transition, it will result in only the destabilization of the native state. In the DSC experiments, as shown in **Figure 4-5**, the Tm of the first transition decreases with rHGH concentration whereas the Tm of the second transition increases with rHGH concentration. A similar behavior is observed in chemical denaturation experiments. In this case the first transition occurs at lower denaturant concentrations and the second transition at higher denaturant concentrations. It is worth mentioning, that several monoclonal antibodies exhibit two chemical denaturation transitions. If this is the case, an assessment of native state aggregation requires that the two transitions exhibit higher ΔG values upon increasing protein concentration.

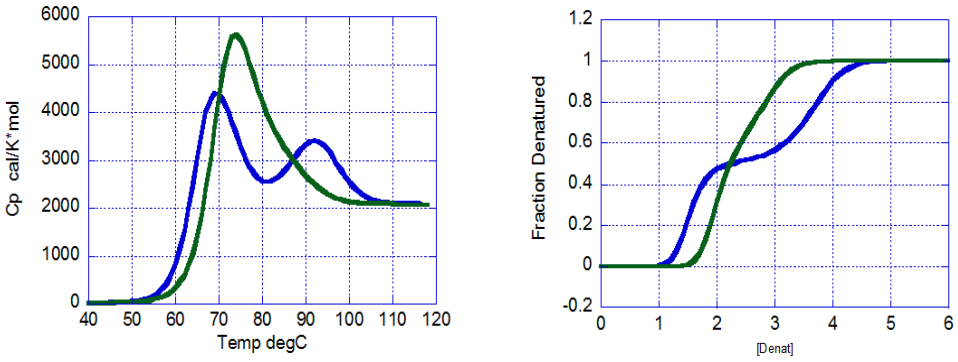

Figure 4-5. Partially denatured state aggregation shifts both transitions in complete protein unfolding. Left panel: The heat capacity function of recombinant human growth hormone at pH 3 (10 mM glycine buffer) as reported by Kasimova et al (*1*). The blue curve corresponds to a concentration of 10mg/mL and the green curve to a concentration of 2mg/mL. Upon increasing concentration (blue curve) the first transition occurs at a lower T_m and the second transition occurs at a higher T_m. Right panel: simulation of expected chemical denaturation of recombinant human growth hormone. Upon increasing protein concentration (blue curve) the first transition is shifted to lower denaturant concentrations (lower ΔG) and the second transition to higher denaturant concentrations (higher ΔG).

Case 3: Denatured State Aggregation

Figure 4-6 illustrates the situation in which denatured state aggregation is present. In this case the equilibrium will be shifted to the right, ΔG will decrease and the stability of the native state will decrease. If this situation occurs, the measured ΔG is given by (*47*):

$$\Delta G_{app} = \Delta G_o^o - RTln(1 + jK_{N,j}[N]^{j-1}) \quad (2)$$

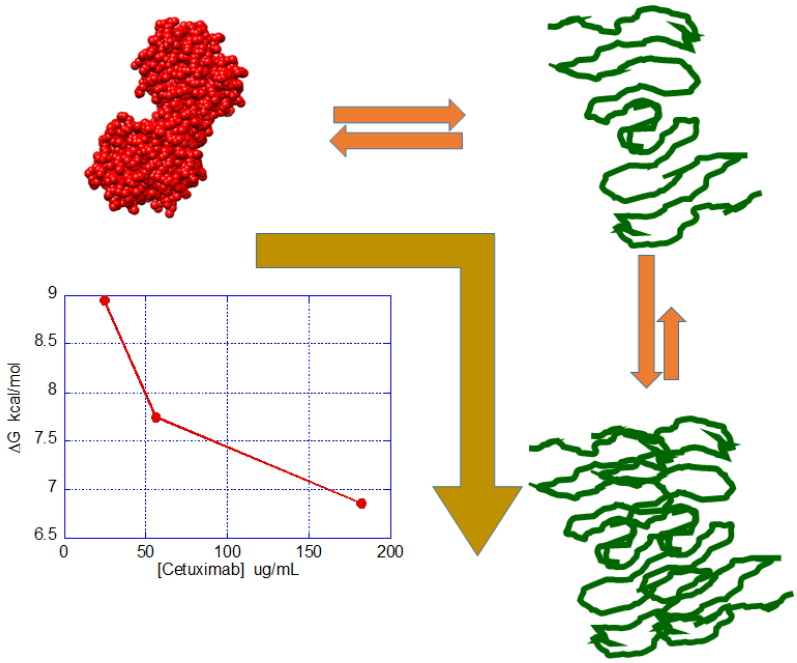

Figure 4-6. Denatured state aggregation will pull the equilibrium to the right and decrease ΔG as the protein concentration increases. Gold arrows indicate direction of equilibrium shift. The decrease in ΔG indicates a lower stability of the native state. The inset illustrates this situation by depicting the concentration dependence of ΔG for Cetuximab in urea denaturation experiments. Denaturation was performed using linear gradient of urea from 0-9 M. The buffer was 10 mM PBS, pH 7.5.

Previously, this behavior has been reported for Cetuximab in urea denaturation experiments (*47*). ΔG decreased from about 9 kcal/mol at 24 μg/mL to 7 kcal/mol at 180 μg/mL consistent with denatured state aggregation. In those experiments, urea was able to resolve only one transition; however, subsequent experiments performed with guanidinium hydrochloride (GndnHCl), a more potent chemical denaturant, were able to resolve two transitions. However, only the first transition exhibited a consistent decrease in ΔG upon increasing antibody concentration suggesting that the aggregating conformation is the partially denatured state emerging from the first transition. The second transition appeared to be independent of concentration further emphasizing that the least stable domain is responsible for the observed aggregation. **Figure 4-7** illustrates this situation. Even though the partially denatured state initiates the

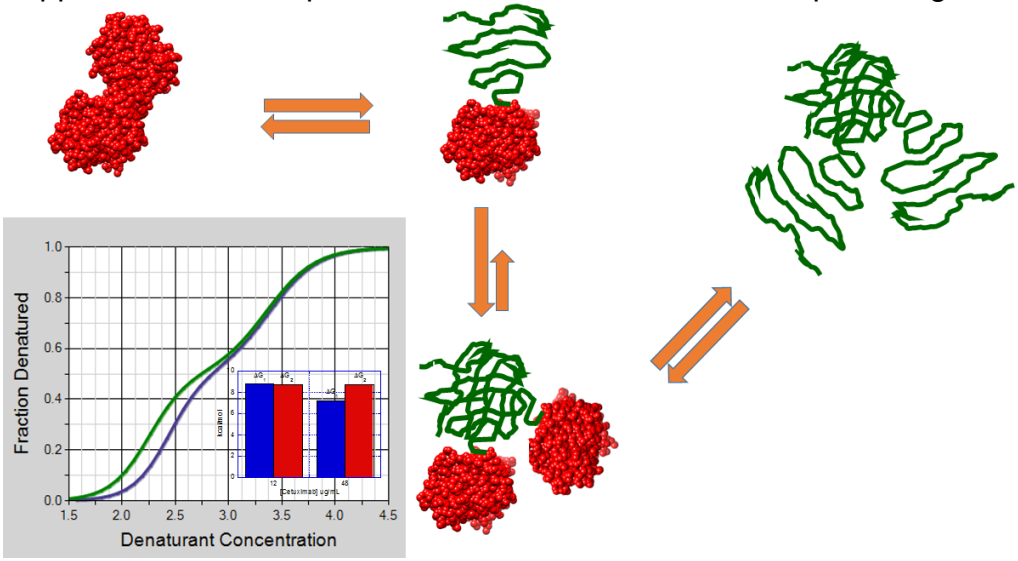

Figure 4-7. Situation in which a partially denatured state exhibits a tendency to aggregate. In this case, full denaturation does not lead to dissociation as in **Figure 4-4**. Even though the denatured high stability domain does not exhibit an intrinsic tendency, the entire protein remains aggregated through the denatured low stability domain. In this situation, the ΔG of the first transition decreases with protein concentration but the second one remains constant. This appears to be the case observed for the guanidinium hydrochloride denaturation of Cetuximab obtained at 12 and 48 μg/mL (inset in the figure). Denaturation was performed using linear gradient of guanidine hydrochloride from 0-5.5 M with same buffer as urea denaturation experiments.

aggregation process, it should not be confused with the situation observed with rHGH in which full denaturation leads to dissociation of the oligomeric intermediates. This dissociation is seen as a ΔG increase for the second transition upon increasing protein concentration. If the Gibbs energy of the second transition remains unchanged, it strongly suggests that the high stability domain does not have an intrinsic aggregating tendency. In this case, measures to prevent aggregation should be aimed towards the least stable domain.

Conclusions

The analysis presented here indicates that different modes of aggregation affect differently the conformational equilibrium of a protein. Since the conformational equilibrium and its concentration dependence can be measured by DSC or ICD, this analysis can provide valuable information in the identification of better protein variants or better formulations. Preventing aggregation processes that are linked to the conformational equilibrium of a protein requires: 1) Minimizing the concentration of aggregating species; and, 2) Minimizing the self-association constant of the aggregating species. This task can be accelerated by a quantitative knowledge of the conformation/self-association equilibrium.

Chapter 5. Preliminary studies on VRC07-523LS

As detailed in Chapter 4, chemical denaturation can be used to determine whether a protein primarily aggregates in the native or denatured state. Comparing the change in ΔG with protein concentration for different buffers can also be a useful tool for formulation development and optimization. An ideal formulation should have a large ΔG with very little dependence on the protein concentration such that at formulation concentrations of 100 mg/mL or greater the protein is maximally stable and shows minimal propensity to aggregate. While excipients like L-Arginine lower the free energy of the native state through their interactions with the denatured state, this interaction also greatly decreases the concentration dependence of the free energy through mitigating aggregation, leading to greater stability at formulation protein concentrations in some cases. It is important to note that if the destabilization of the native state is great enough, the value of ΔG at high protein concentrations may still be lower than for other formulations with more of a concentration dependence. Chemical denaturation studies at a range of protein concentrations were conducted with VRC07 in 4 buffers which were identified as potential formulation buffers at the VRC during development

Figure 5-1. ΔG values for VRC07 at different protein concentrations using GdnHCl as denaturant. Values were calculated using parameters obtained by a global fit of concentration dependence data with a 0-6.4M gradient of GdnHCl.

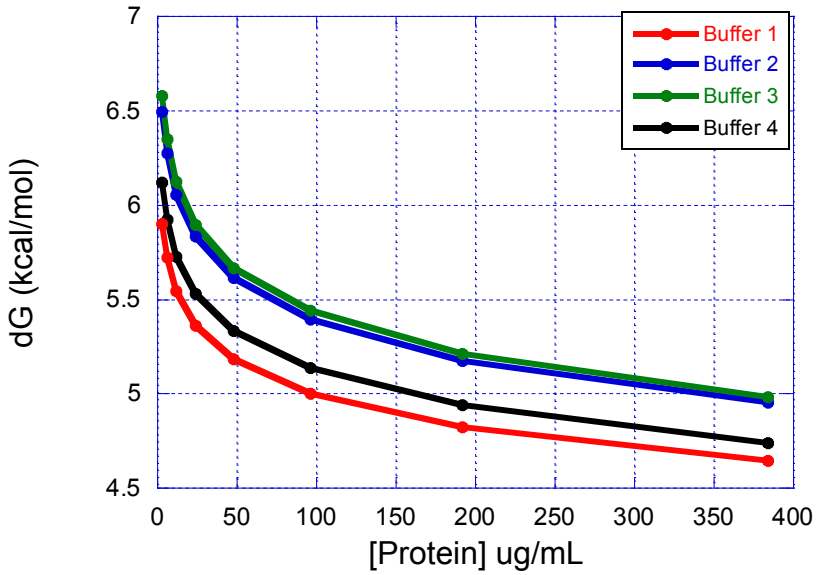

of VRC07: buffer/formulation 1 (50 mM histidine, 100 mM NaCl, pH 6.8), buffer/formulation 2 (50 mM histidine, 100 mM NaCl, 5% w/v sucrose, pH 6.8), buffer/formulation 3 (50 mM histidine, 100 mM NaCl, 5% w/v sorbitol, pH 6.8), and buffer/formulation 4 (50 mM histidine, 50 mM NaCl, 5% w/v sucrose, 2.5% w/v sorbitol, pH 6.8). These experiments showed very little difference in stability between the four buffers, as shown by their similar ΔG values at different protein concentrations, as well as a decrease in stability with increasing protein concentration indicating denatured state aggregation (**Figure 5-1).** These ΔG values were calculated using parameters obtained from global fits of the concentration dependence data for each buffer. Since these global fits rely on numerous parameters obtained from the data, not all of which are always reliable to determine, it is often useful to analyze chemical denaturation data using the concentration at which half of the protein is denatured, or $C_{1/2}$, as this value is less dependent on the shape of each individual curve and the resulting native and denatured baselines and is therefore extremely reliable and replicable between experiments. The reliability of these other parameters, such as the slope of the transition region or m-value, can usually be improved by obtaining more data points in each denaturation curve, although this requires significantly more protein for each curve. **Figure 5-2** shows a plot of $C_{1/2}$ vs protein concentration which clearly shows that Buffer 4 is the best performing buffer

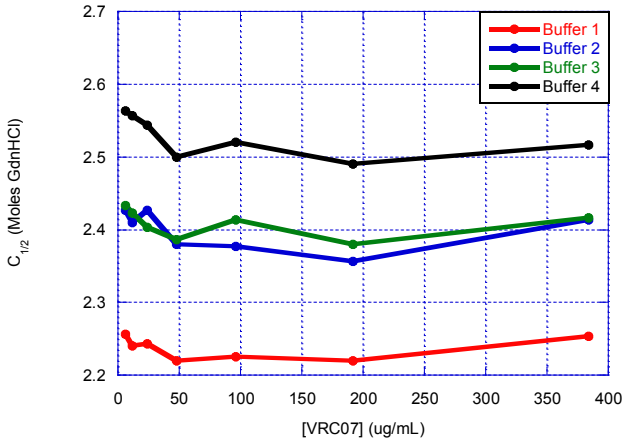

Figure 5-2. $C_{1/2}$ vs protein concentration for VRC07 as measured using GdnHCl as denaturant. Conditions are same as Figure 5-1.

with the largest $C_{1/2}$ values at every tested protein concentration, while buffer 1 is the worst of the set.

DSC studies are also useful in formulation development as detailed in Chapter 1, but investigations of monoclonal antibody stability are often impeded by the irreversibility of antibody thermal unfolding transitions, precluding a full thermodynamic analysis of the curves and even affecting their shape and properties. To attempt to address this issue, various DSC experiments were conducted with VRC07 looking at the effect of pH and low concentrations of GdnHCl on the reversibility of unfolding transitions. At formulation pH (6.8), the DSC thermogram for VRC07 shows one peak centered at 70°C, but when the pH is decreased to 3.5, three distinct transitions appear as shown in **Figure 5-3A**. Reversibility for a transition was tested by scanning to a temperature just past the T_m, then

Figure 5-3. Decreasing pH to 3.5 reveals three separate transitions in VRC07 thermal unfolding. **A)** DSC thermograms for 1 mg/mL VRC07 in pH 6.8 (20 mM sodium phosphate) and 3.5 (50 mM sodium formate, 50 mM NaCl) buffer at 1°C/min scan rate. The scan at pH 6.8 has one peak at 70.8°C, while the scan at pH 3.5 has peaks at 40.3, 55.6, and 90.6°C. **B)** DSC scan showing the reversibility of each transition for 1 mg/mL VRC07 at pH 3.5. A full scan is shown for reference, after which the instrument was cleaned and reloaded with protein and the reversibility of each transition was tested as described in the text.

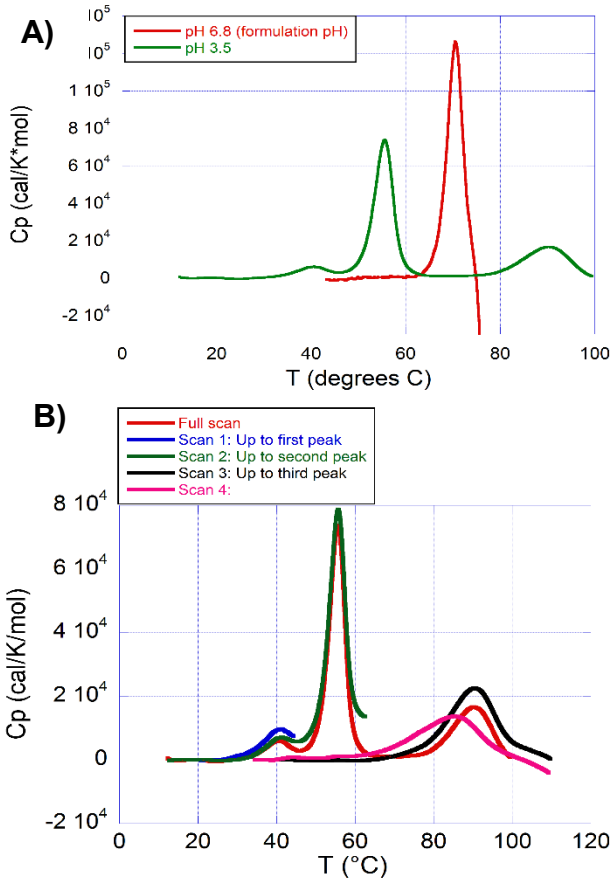

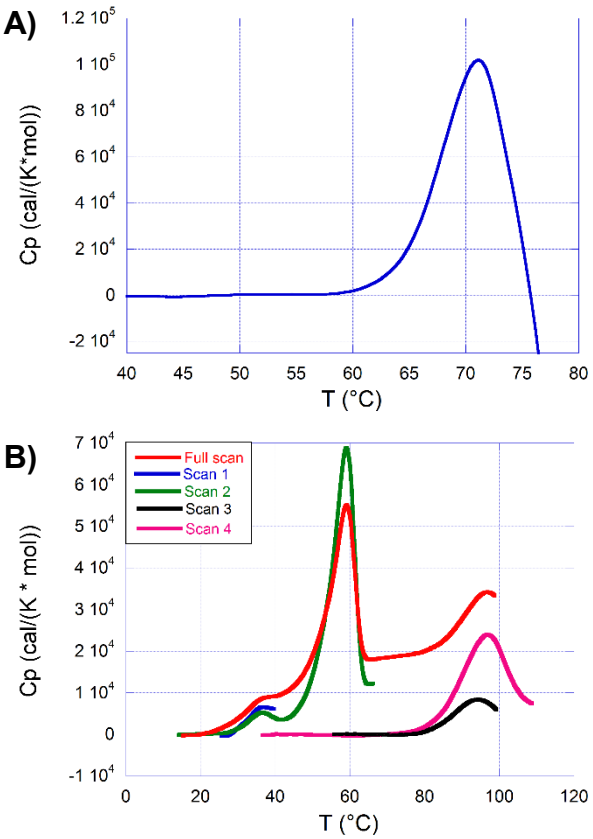

Figure 5-4. Decreasing pH to 3.5 reveals three separate transitions in VRC01 thermal unfolding. **A)** DSC thermogram for 1 mg/mL VRC01 in formulation buffer (pH 5.8, 25 mM sodium citrate, 50 mM NaCl, 50 mM L-Arginine) at 1°C/min scan rate. The one peak is centered at 71.2°C. **B)** DSC scan showing the reversibility of each transition for 1 mg/mL VRC07 at pH 3.5. A full scan is shown for reference, after which the instrument was cleaned and reloaded with protein and the reversibility of each transition was tested as described in the text. The three peaks are centered at 37, 59.3, and 97°C. The first and third transition are reversible.

cooling the instrument back to the starting temperature, then scanning all the way through the given transition. If the transition is reversible, the rescan will contain a peak at that temperature, while an irreversible transition will show no signal upon rescanning. As shown in **Figure 5-3B**, the first transition is fully reversible, the second transition is irreversible, and the third transition appears to be partially reversible judging by the decreased T_m and enthalpy of the peak upon rescanning. Interestingly, in appearance of three transitions at pH 3.5 was also observed for two other tested mAbs: VRC01LS and Cetuximab. VRC01LS is another therapeutic HIV

antibody developed at the NIH as briefly discussed in Chapter 1 and 6 of this work, while Cetuximab (trade name Erbitux) is an anti-EGFR antibody used in the treatment of various cancers (*48*). Both antibodies, particularly Cetuximab, are somewhat difficult to formulate. They also both have one unfolding transition at their formulation pH, but show three distinct transitions at pH 3.5 where the first and third transition are at least somewhat reversible. These thermograms are shown in **Figure 5-4** (VRC01) and **Figure 5-5** (Cetuximab).

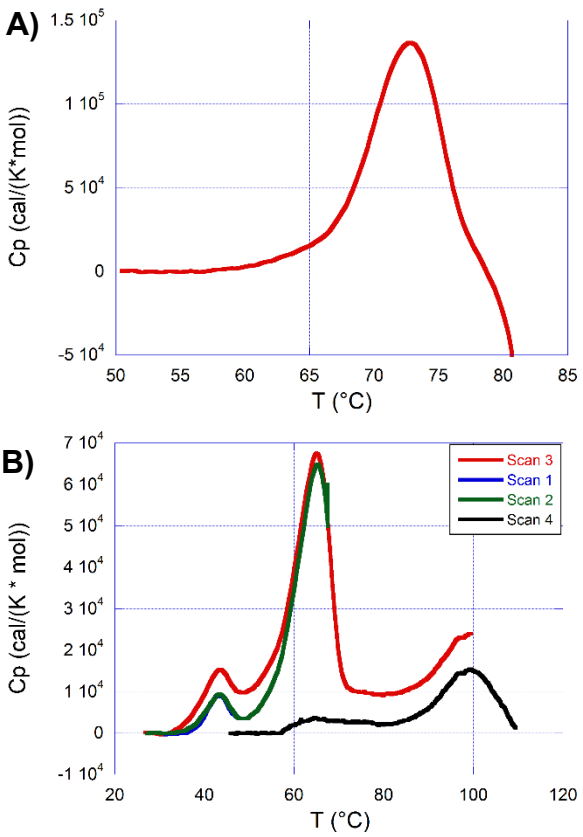

Figure 5-5. Decreasing pH to 3.5 reveals three separate transitions in Cetuximab thermal unfolding. **A)** DSC thermogram for 1 mg/mL Cetuximab in formulation buffer (pH 7.5, 10 mM PBS) at 1°C/min scan rate. The one peak is centered at 72.8°C followed by sample precipitation. **B)** DSC scan showing the reversibility of each transition for 1 mg/mL VRC07 at pH 3.5. The three peaks are centered at 43.6, 65, and 99.4°C. The first and third transition are reversible.

Chapter 6. Long-Term Stability of an HIV-1 Neutralizing Monoclonal Antibody Using Isothermal Calorimetry.

This chapter was published in Analytical Biochemistry (Clarkson et. al. 2018).

Abstract

Different factors affect the long term stability of monoclonal antibodies, among them denaturation or partial denaturation that is often followed by aggregation. Isothermal calorimetry is capable of quantifying the kinetics of denaturation/aggregation

of an antibody by measuring the heat that is released or absorbed by the process over a period of days or weeks, at temperatures below its denaturation temperature, T_m. The denaturation/aggregation kinetics of the anti-HIV monoclonal antibody VRC07-523LS was measured by isothermal calorimetry at different concentrations in four different formulation buffers. The measurements were performed at ten degrees below T_m, as determined by differential scanning calorimetry. The formation of aggregates was also followed by size exclusion chromatography at 5°C, 25°C and 40°C over a period of 8-36 weeks. It was observed that the rates measured by isothermal calorimetry correlate quantitatively with those measured by size exclusion chromatography. Since isothermal calorimetry experiments are performed over a period of ten days, it can become a valuable tool for a fast prediction of the best formulations.

Introduction

VRC01 is a highly potent CD4-binding monoclonal antibody that neutralizes ~90% of HIV-1 strains with an IC_{50} of less than 50 µg/ml (*49*). VRC07-523LS is a more potent clonal relative of VRC01 with 5 - 8-fold increased potency *in vitro*. In nonhuman primates, VRC07-523LS prevented infection at a 5-fold lower concentration than VRC01 (*32*). These monoclonal antibodies are being developed by the Vaccine Research Center at the National Institutes of Health as immunotherapeutic agents for the suppression of acute HIV replication. Nevertheless, future clinical use of VRC07-523LS or a similar monoclonal antibody, would require a dose on the order of 1 - 10mg of monoclonal antibody per kg of body weight. Dosages of that magnitude require formulations with protein concentrations on the order of 100mg/mL or greater.

Formulating a monoclonal antibody at 100mg/mL or even higher concentrations gives rise to different challenges, including maintaining the structural stability of the antibody and minimizing any tendency to aggregate over long periods of time (*13, 50*). Identifying the best buffer and excipient conditions that maximize the long term stability of a monoclonal antibody is a major goal in biologics research. It has become evident that not a single technique is sufficient for accurate decisions and that researchers need to rely on a battery of orthogonal measurements (*51, 52*). Two types of techniques are generally available, techniques with the potential to quickly identify and predict the top formulation conditions (e.g., differential scanning calorimetry, differential scanning fluorometry, isothermal chemical denaturation) and techniques that actually measure aggregation after sample incubation for a relatively long period of time (e.g., size exclusion chromatography, light scattering). For these techniques, the incubation times are usually reduced by accelerating any aggregation process by, for example, increasing the incubation temperature or stressing the sample in different ways (*53-56*). Often, results obtained from accelerated conditions do not correlate with aggregation pattern observed by SEC especially at lower temperatures.

In this paper, we have utilized isothermal calorimetry as a novel technique to measure the kinetics of denaturation/aggregation of a monoclonal antibody (VRC07-523LS), and compare the results with those obtained by size exclusion chromatography (SEC). Isothermal calorimetry, not to be confused with isothermal titration calorimetry (ITC), measures the rate of heat production or absorption associated with a spontaneous process occurring at a given temperature over relatively long periods of time, weeks or more. For example, a protein that denatures and/or aggregates upon

storage at constant temperature, will absorb or release heat as a function of time in an amount proportional to the rate of increase in the concentration of denatured and/or aggregated protein. Since the instrument is capable of measurements during days - to - weeks, isothermal calorimetry appears to be ideal to determine the rate of denaturation/aggregation at temperatures below the denaturation temperature (T_m) of proteins.

In this paper, the kinetics of denaturation/aggregation of the monoclonal antibody VRC07-523LS has been measured by isothermal calorimetry at temperatures below T_m for four different formulation buffers. Additional size exclusion chromatography experiments (SEC) indicate that the isothermal calorimetry experiments provided an identical rank order for the buffers considered in this study.

Materials and Methods

Proteins and Reagents: The VRC/NIAID/NIH Vaccine Production Program (VPP) laboratory, Gaithersburg. MD, has developed optimized cell lines, upstream expression systems, and downstream purification processes for the VRC07-523LS monoclonal antibody. Expression methods employ scalable, optimized fed-batch culture of stably-transfected Chinese Hamster Ovary (CHO) DG44 cells with termination by culture supernatant harvest. Purification by chromatography incorporates two orthogonal methods, a typical Protein A affinity capture step and a negative-capture with Capto Adhere (GE Healthcare), a multimodal polishing resin engineered specifically for Protein A-purified proteins. Viral clearance is accomplished via low pH and viral filtration. Processing is concluded by diafiltration into formulation buffer and a final sterile

filtration. Four formulation buffers for VRC07-523LS were developed at the VRC/NIAID/NIH Vaccine Production Program (VPP) laboratory using design of experiment studies for optimizing pH, ionic strength, and buffer salt composition. Excipients which are either “Generally Regarded As Safe” (GRAS) by the FDA or have known acceptable safety profiles were screened using multiple techniques for determining colloidal and conformational stability to identify potential stabilizers. The buffers identified were formulation 1 (50 mM histidine, 100 mM NaCl, pH 6.8), formulation 2 (50 mM histidine, 100 mM NaCl, 5% w/v sucrose, pH 6.8), formulation 3 (50 mM histidine, 100 mM NaCl, 5% w/v sorbitol, pH 6.8), and formulation 4 (50 mM histidine, 50 mM NaCl, 5% w/v sucrose, 2.5% w/v sorbitol, pH 6.8). Protein solutions at ~150 mg/mL were dialyzed overnight against the desired buffer and diluted to the measuring concentration of 100, 50 or 25 mg/mL (isothermal calorimetry experiments), or ~1-2 mg/mL (DSC experiments). Chemicals for buffer preparation were purchased from multiple vendors: L-Histidine (98%, CAS 71-00-1) from Acros Organics (New Jersey, USA), NaCl (Certified ACS/Crystalline, CAS 7647-14-5) from Fisher Scientific (Fair Lawn, NJ, USA), and sucrose (minimum 99.5%, CAS 57-50-1) and D-sorbitol (minimum 98%, CAS 50-70-4) from Sigma-Aldrich (St. Louis, MO, USA).

Size Exclusion Chromatography: High performance size exclusion chromatography (HPSEC) was used to monitor the levels of aggregation and fragmentation. Samples were analyzed using a ACTUITY BEH200 column (Waters) and 2X Phosphate Buffer Saline as the mobile phase. The monomer peak percentage was calculated as the monomer peak area divided by the total area of all protein related peaks. The peak area of all peaks eluting at times earlier than the monomer peak were reported as percent

aggregate. Peaks eluting after the monomer peak, if present, were reported as percent fragment.

Differential Scanning Calorimetry: Thermal denaturation experiments were performed using both a VP-DSC microcalorimeter with a standard "lollipop" cell, as well as a VP-DSC capillary cell microcalorimeter, from MicroCal/Malvern Instruments (Northamption, MA, USA) with scans from 10 to 100°C at a rate of 1°C/min. Dialyzed protein was diluted to ~1 mg/mL (standard cell) and ~2 mg/mL (capillary cell), thoroughly degassed, then loaded into the calorimetric cell (~0.5 and ~0.12 mL in volume respectively). The reference cell was filled with dialysis buffer. Data collection and processing were performed using the software included with the instruments. Data analysis was performed using the equations previously described in the literature for irreversible DSC protein denaturation (*57, 58*). These equations were introduced into the DataFit software package (Oakdale Engineering, Oakdale, PA, USA).

Isothermal Calorimetry: Isothermal calorimetry experiments were performed using a TAM IV microcalorimeter system from TA Instruments (New Castle, DE, USA) equipped with six calorimeter channels as described previously (*59, 60*). The experiments were conducted at 60°C. Before samples were inserted, an initial 30-minute baseline was recorded. Cylindrical glass ampoules were filled with 1 mL of protein solutions or buffer, and were hermetically sealed with crimp caps. The ampoules were then loaded into each calorimetric channel to a position where they are allowed to equilibrate to the instrument temperature for 45 minutes before being lowered into the measuring position. The heat flow, dQ/dt, was recorded as a function of time until all processes had gone to completion and the signal stabilized at a level close to zero (~ 8 days).

After removing the samples from the instrument, a final 30-minute baseline was recorded. The baseline from the empty calorimeters were subtracted from the data collected for each. The signal from the ampoule containing only buffer was subtracted from the heat flow from the sample and the differential signal was normalized per mole of protein. The final signal was expressed as kcal/day/mol. Data collection and processing of raw data were performed using the software included with the instrument. Analysis of the isothermal calorimetry data was performed using the equations described in this paper. These equations were introduced into the DataFit software package (Oakdale Engineering, Oakdale, PA, USA).

Results and Discussion

Differential Scanning Calorimetry. **Figure 6-1** shows the temperature dependence of the heat capacity function (C_p) of VRC07-523LS in the four buffers studied. These experiments were performed in a standard "lollipop" shaped cell microcalorimeter. For the four buffers studied, the denaturation of VRC07-523LS is clustered around 70°C. The temperature denaturation of VRC07-523LS is irreversible and characterized by an endothermic peak, associated with unfolding, immediately followed by a large

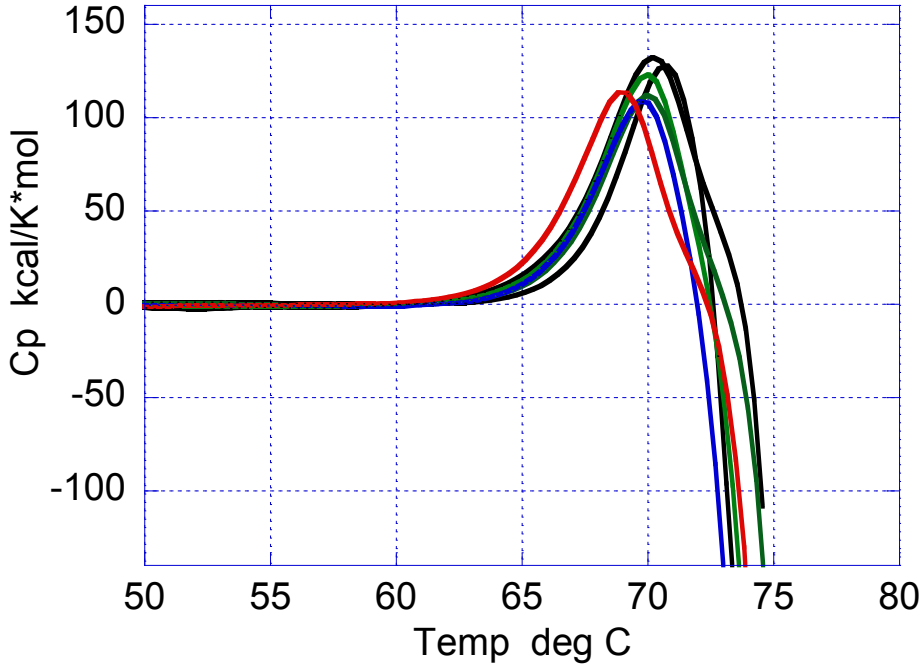

Figure 6-1. The temperature dependence of the heat capacity function of VRC07-523LS in the four formulation buffers studied, measured by a standard cell microcalorimeter in duplicate: red: buffer 1; blue: buffer 2; green: buffer 3; black: buffer 4.

exothermic effect associated with aggregation and precipitation. As noted before and shown in **Figure 6-2** the calorimetric scans obtained in a DSC instrument equipped with capillary cells have no visible exothermic peak. This phenomenon has been known for over thirty years (*25, 26*) and appears to be related to the shorter travel path experienced by the sample when it aggregates and precipitates. The absence of the aggregation/precipitation exotherm in the capillary cell DSC reveals the presence of the additional denaturation peaks of the monoclonal antibody, and the possibility of analyzing the entire denaturation process. Also, since the exotherm is not present a much higher reproducibility of the data is achieved. Since the denaturation of VRC07-523LS is irreversible, the heat

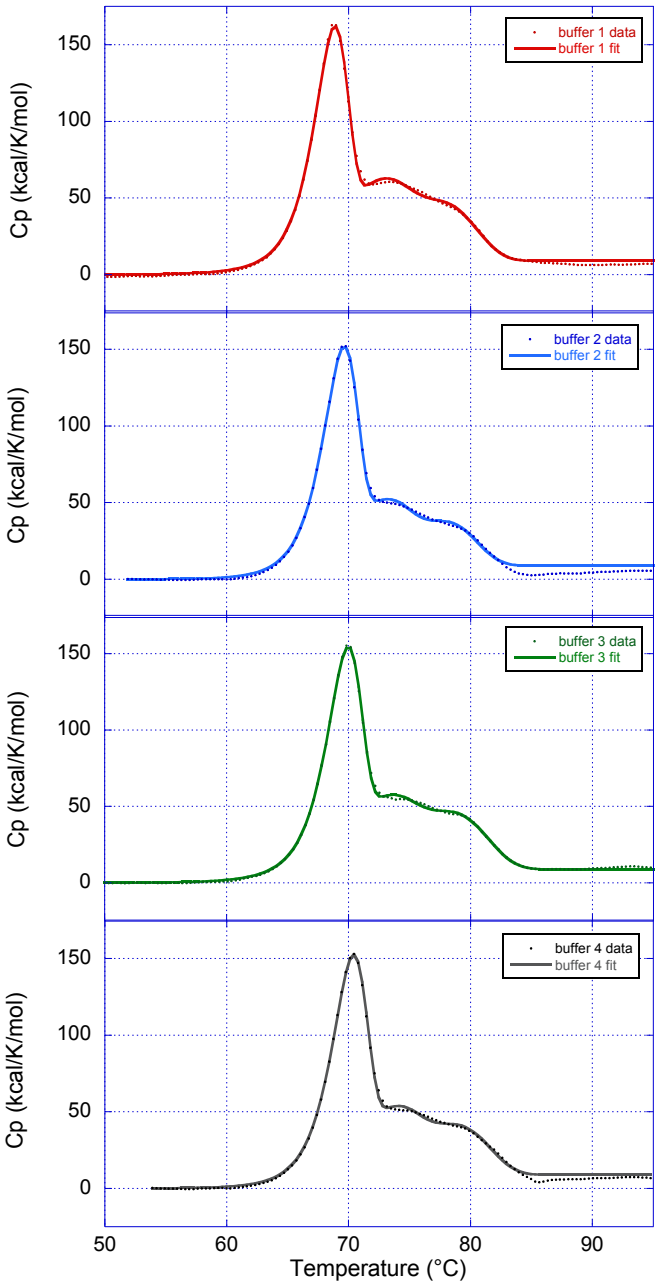

Figure 6-2. The temperature dependence of the heat capacity function of VRC07-523LS in the four formulation buffers studied, measured by a capillary cell microcalorimeter: red: buffer 1; blue: buffer 2; green: buffer 3; black: buffer 4. In this figure, the solid lines for each curve represent the results of the analysis of the heat capacity data to the sum of three irreversible transitions (see text for details).

capacity data was deconvoluted in terms of a sum of kinetically controlled irreversible transitions (*57, 58*). For all four buffers, the heat capacity data could be well accounted for by three separate transitions.

The data as well as the calculated heat capacity curves are shown in **Figure 6-2**. Each transition is characterized by a T_m, a calorimetric enthalpy change (ΔH) equal to the area under each peak and an activation enthalpy ($\Delta H^{\dagger}$) responsible for the temperature dependence of the rate of denaturation. Irreversible transitions are kinetically controlled and their T_m is determined by the temperature acceleration of the rate of denaturation (*57, 58*). The parameters obtained by non-linear least squares analysis of the heat capacity function for all four buffers are summarized in **Table 6-1**. The T_m of the main transition peak is centered around 70°C and increases from buffer 1 through buffer 4. It must be noted that the total increase is only 1.5°C and even less between some buffers, a difference that can be easily missed in the early stages when the antibody preparation has not been optimized. The same situation is observed for the other transitions as

Table 6-1

Deconvolution of Heat Capacity Function of VRC07-523LS *

Tm's are in °C, the calorimetric enthalpies (ΔH's) are in kcal/mol and the activation energies $\Delta H^{\dagger}$'s are in kcal/mol.

Buffer	Tm1	Tm2	Tm3	$\Delta H1$	$\Delta H2$	$\Delta H3$	$\Delta H_1^{\dagger}$	$\Delta H_2^{\dagger}$	$\Delta H_3^{\dagger}$
1	68.7	71.9	77.2	462.0	121.4	369.8	173.9	81.93	70.1
2	69.5	72.4	77.7	459.0	117.4	238.7	169.2	91.9	81.0
3	69.8	72.5	78.1	445.2	112.2	365.4	169.7	83.6	69.2
4	70.3	73.1	78.4	461.4	109.7	302.9	167.7	90.8	73.2

shown in **Table 6-1**. Judging by the T_m values, the rank order of conformational stability is buffer 4 > buffer 3 > buffer 2 > buffer 1. The main transition is characterized by an enthalpy change of ~460 kcal/mol and the smaller transitions by enthalpies averaging 115 and 320 kcal/mol respectively. Perhaps, more importantly, the activation enthalpy of the main transition averages 170 kcal/mol whereas those of the two smaller peaks average 87 and 73 kcal/mol respectively. Since the temperature dependence of the rate of denaturation is determined by the activation enthalpy (a smaller positive activation enthalpy means a smaller decrease in the rate at lower temperatures, $d\ln k/dT = \Delta H^{\dagger}/RT^2$, see equation 7) the DSC data suggest that at low temperatures the smaller transitions might precede the main transition. If this is the case and the activation heat capacities do not alter the trend, these results would suggest that the two smaller transitions, which are potentially the CH2 and CH3 domains (*61, 62*), may be the ones that denature and aggregate first at low temperatures.

With the microcalorimeter equipped with standard “lollipop” cells **(Figure 6-1)**, only the main denaturation peak (T_m) is visible and centered at 69.2 ± 0.2 °C for buffer 1, 69.9 ± 0.1 for buffer 2, 69.9 ± 0.1 for buffer 3 and 70.5 ± 0.2 for buffer 4 which is close to the location of the main peaks measured by the capillary DSC. Since the calorimetric signal in the non-capillary DSC instrument is composed of two terms of opposite sign, an endotherm due to unfolding and an exotherm due to aggregation/precipitation, the exact location of the peak maximum depends on the exact separation between the two events which is not necessarily the same under all conditions or even separate experiments (*63*). Nevertheless, inspection of the data

reveals a shoulder around 72.5 – 73.5°C probably due to the first minor peak and this shoulder immediately precedes the aggregation/precipitation exotherm.

Isothermal Calorimetry. Isothermal calorimetry (not to be confused with isothermal titration calorimetry) measures the rate at which heat is released or absorbed (heat flow) by a spontaneous process at constant temperature. The irreversible denaturation of proteins is a kinetically controlled process (*58, 64-66*). At low temperatures the rate of the reaction is extremely slow and becomes progressively faster as the transition temperature is approached. For the initial isothermal calorimetry experiments, it is important to select a temperature at which the reaction occurs with an optimal rate for accurate measurements; i.e. hours to weeks. If the temperature is too high and the reaction occurs within minutes or less, the sample will not be able to equilibrate and the measurement will be impossible. On the other hand, if the temperature is too low and the reaction too slow, the rate of

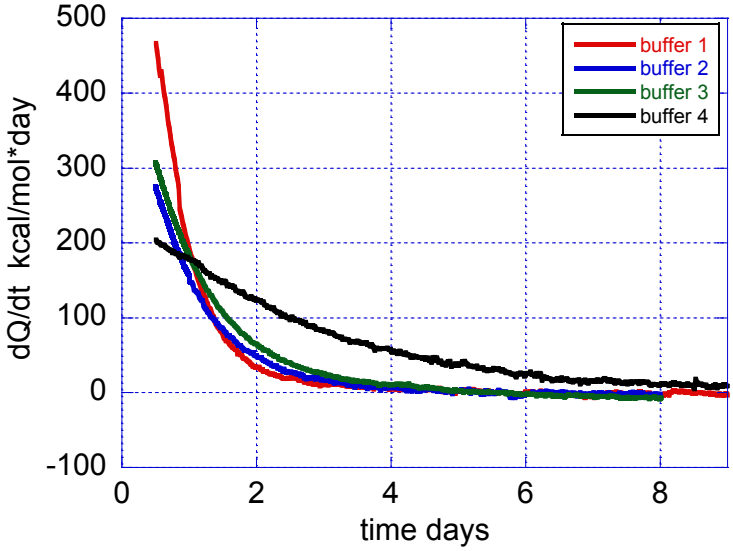

Figure 6-3. Heat flow (dQ/dt) recorded as a function of time for VRC07-523LS in the four formulation buffers studied: red: buffer 1; blue: buffer 2; green: buffer 3; black: buffer 4. The experiment was performed at 60°C at a protein concentration of 100 mg/mL in a volume of 1.0 mL. The curves in the graph were obtained after subtraction of the signal from an ampoule containing buffer run in parallel followed by normalization by the amount of protein. In this figure, a positive heat flow corresponds to an endothermic process.

heat production or absorption will be lower than the detection limits of the instrument. A good rule of thumb is to perform the first experiments at a temperature 10 degrees below T_m, at which the reaction is expected to proceed and complete in several days (*59*). The temperature for the initial VRC07-523LS isothermal calorimetry experiments was set at 60°C.

Figure 6-3 shows the normalized heat flow for VRC07-523LS at the desired formulation concentration of 100mg/mL at 60°C for the four buffers in this study. All of them display an endothermic (positive signal) heat event that decreases monotonically until the baseline level is reached. None of the curves goes below zero, as would have been the case if aggregation were slower than denaturation and the two processes were separated in time as shown previously (*59*). For VRC07-523LS, it appears that the two processes (denaturation and aggregation) occur very close to each other and that only a composite curve is observed. Total aggregation of the samples after conclusion of the experiments (9 days) was confirmed by visual inspection. Examination of the data in **Figure 6-3** immediately reveals that buffer 1 exhibits the fastest rate of denaturation/aggregation while buffer 4 the slowest one. Buffers 2 and 3 exhibit intermediate rates, buffer 2 exhibiting slightly faster denaturation than buffer 3. Additionally, the total heat measured by isothermal calorimetry is 540 ± 67 kcal/mol which is less than the 890 ± 60 kcal/mol total denaturation enthalpy measured by the capillary DSC. Since the isothermal calorimetry measurement is ten degrees below T_m, this difference could be due to the heat capacity of denaturation of the antibody. However, the only ΔC_p reported in the literature for the denaturation of a monoclonal antibody is by Lazar et al (*67*) who determined a ΔC_p of 8 kcal/K*mol by chemical

denaturation experiments performed at different temperatures. If we use the ΔC_p value determined by Lazar et al, the expected denaturation enthalpy at 60°C would be 810 kcal/mol which is still higher than the 540 kcal/mol measured by isothermal calorimetry. Alternatively, if the ΔCp values measured for smaller proteins are extrapolated to the molecular weight of an antibody, a ΔCp of 18 kcal/K*mol could be expected (*68*), in which case the enthalpy at 60°C would amount to 710 kcal/mol, also higher than the value measured by isothermal calorimetry. If these values bracket the actual ΔCp, we can estimate that the heat of aggregation for VRC07-523LS is on the order of -170 - -270 kcal/mol, which is exothermic as expected.

*Isothermal Calorimetry Data Analysis***.** The heat associated with the unfolding followed by aggregation of the protein, relative to that of the native non-aggregated protein is proportional to the populations of denatured and aggregated protein. In general, at any degree of unfolding and aggregation of the unfolded state, the heat, Q_{Total}, is equal to:

$$Q_{Total} = \Delta H_u v[P_u] + Q_{agg} v[P_{agg}] \quad (1)$$

Where v is the sample volume, $[P_u]$ and $[P_{agg}]$ are the concentration of denatured (unfolded) and aggregated protein respectively. ΔH_u and Q_{agg} are the molar heats of unfolding and aggregation respectively. Equation 1 can be written in terms of the total

protein concentration and the fractions of unfolded, F_u, and unfolded aggregated, F_{agg}, protein as follows:

$$Q_{Total} = \Delta H_u v[P_t]F_u + Q_{agg} v[P_t]F_u F_{agg} \quad (2)$$

The measured heat is normalized with regard to the amount of protein in the calorimetric cell:

$$Q = \frac{Q_{Total}}{v[P_t]} = \Delta H_u F_u + Q_{agg} F_u F_{agg} \quad (3)$$

Since denaturation/aggregation are kinetic processes, the fractions of unfolded and aggregated protein can be written in terms of the rates of unfolding and aggregation as:

$$Q = \Delta H_u(1 - e^{-k_u t}) + Q_{agg}(1 - e^{-k_u t})(1 - e^{-k_{agg} t}) \quad (4)$$

Finally, the quantity directly measured by isothermal calorimetry is the time derivative of the heat absorbed or released by the reaction and referred to as heat flow, $q = dQ/dt$,

$$q = k_u \Delta H_u e^{-k_u t} + k_{agg} Q_{agg} e^{-k_{agg} t} + k_u Q_{agg} e^{-k_u t} - (k_u + k_{agg}) Q_{agg} e^{-(k_u + k_{agg}) t} \quad (5)$$

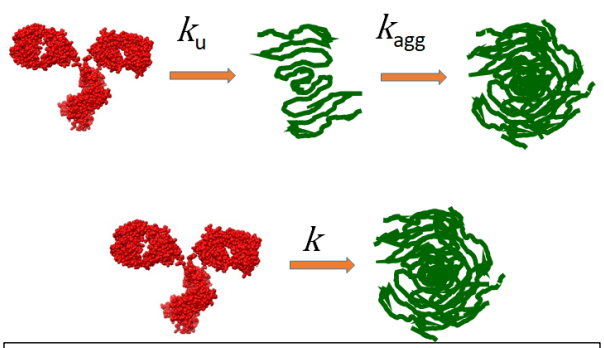

Figure 6-4. Schematic diagram showing two different situations for a denaturation/aggregation reaction. In the top panel, the rate of denaturation or partial denaturation is faster than the rate of aggregation resulting in two separated and observable reactions. If the rate of aggregation is much faster than the rate of denaturation, the two reaction collapse into a single transition characterized by a single rate constant.

Equation 5 accounts for the situation depicted in **Figure 6-4** (top panel) in which the protein denatures or partially denatures and then aggregates. If $k_{agg} >> k_u$ the two processes will occur at once and characterized by a single apparent rate constant (**Figure 6-4** bottom panel). In this case, the total heat is the sum of the unfolding and aggregation heats. Equation 5 reduces to:

$$q = k_u (\Delta H_u + Q_{agg})\, e^{-k_u t} = k_u Q_{total} e^{-k_u t} \quad (6)$$

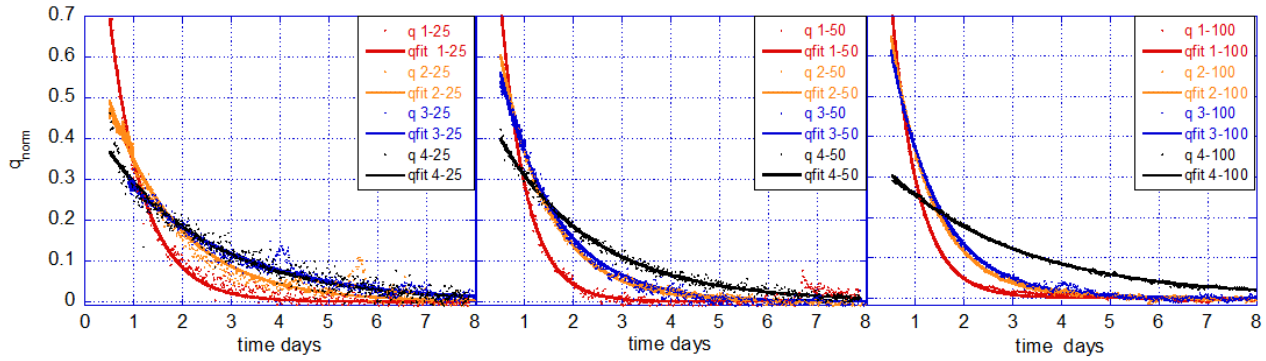

Figure 6-5. Non-linear least squares fits of the heat flow versus time data for VRC07-523LS at three different concentrations in the four formulation buffers studied. For illustration purposes, the heat flow normalized by the total heat, q_{norm}, has been plotted in the figure. The denaturation/aggregation rates determined by non-linear least squares to equation 6 are shown in **Figure 6-6**.

Equation 5 was used to analyze the VRC07-523LS the isothermal calorimetry data. It became immediately apparent that all the data was well accounted by a single exponential as described by equation 6. **Figure 6-5** shows the VRC07-523LS isothermal calorimetry data obtained at 60°C for the concentrations of 25, 50 and 100mg/mL in the four buffers studied in this report as well as the results of the non-linear least squares fits. As expected, the signal-to-noise ratio is lower at the lower concentrations studied and illustrates the goodness of the data that can be obtained with monoclonal antibodies at different concentrations. In formulation evaluation analysis, obtaining data at the formulation concentration (100mg/mL or even higher) is critical since most techniques require the use of much lower concentrations that can skew the results. Also, since isothermal calorimetry can be performed at lower concentrations, it should be a good screening tool to establish the range of concentrations that provide accurate stability answers.

Denaturation/Aggregation Rates at 60°C. **Figure 6-6** shows the denaturation/aggregation rates obtained from the analysis of the data in **Figure 6-5**. It is clear that the best buffer according to the isothermal calorimetry experiments is buffer 4 (k = 0.4 days^{-1} at 100mg/mL) and that buffer 1 (k = 1.8 days^{-1} at 100mg/mL) is the worst. Buffer 2 and 3 occupy a close intermediate position but buffer 3 (k = 0.76 days^{-1} at 100mg/mL) appears to be better as it displays lower rates than buffer 2 (k = 0.9 days^{-1} at 100mg/mL) at all protein concentrations. It is noteworthy that for buffers 2 and 3 and apparently also for buffer 1, the rates appear to increase with protein concentration. Unfolding by itself is a monomolecular reaction and therefore independent of concentration. Aggregation, on the other hand, is concentration dependent and its rate is expected to increase at higher concentrations, suggesting that in these two buffers the rates of aggregation and denaturation are closer in magnitude.

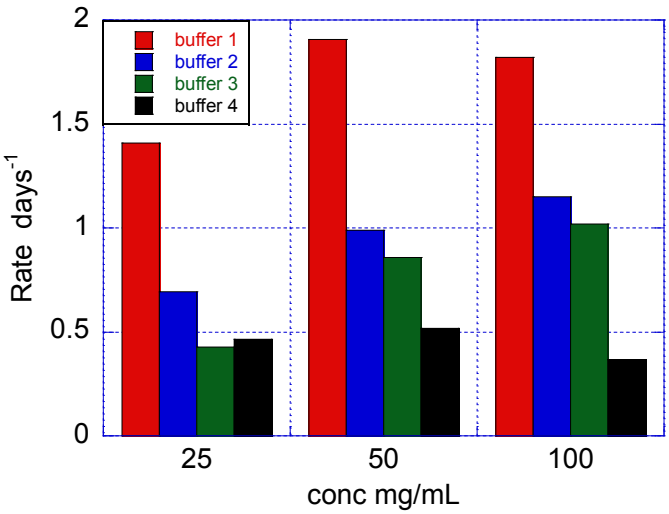

Figure 6-6. The denaturation/aggregation rates for VRC07-523LS determined by isothermal calorimetry at three different concentrations in the four formulation buffers studied at 60°C.

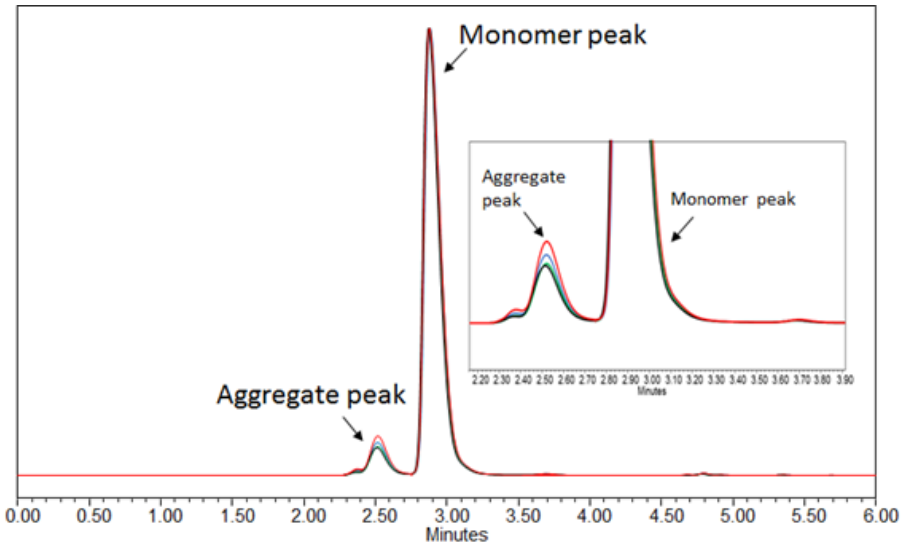

Figure 6-7. Representative SEC chromatograms of VRC07-523LS in the four formulation buffers after 12 weeks storage at 25°C: red: buffer 1; blue: buffer 2; green: buffer 3; black: buffer 4. The inset shows zoomed in image of the aggregate peak.

Size Exclusion Chromatography. VRC07-523LS was dialyzed into the four different buffers at a final concentration of approximately 100 mg/mL. The antibody was then stored for 9 months at 5°C and 3 months at 25°C and 40°C and samples were tested at different intervals for change in aggregate content (see Materials and Methods). **Figure 6-7** shows a representative chromatogram obtained after 12 weeks storage at 25°C**. Figure 6-8** shows the SEC data obtained at 5°C, 25°C and 40°C for several weeks. In this figure the percent monomer population has been plotted as a function of time. It is evident that at all temperatures the rate of aggregation is faster in buffer 1 while the slowest

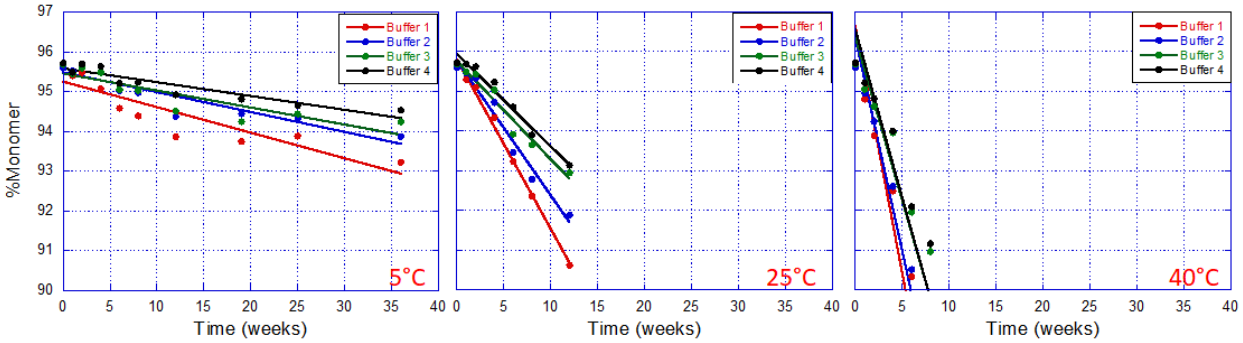

Figure 6-8. Per cent VRC07-523LS in monomeric form measured by size exclusion chromatography (SEC) as a function of time at 5, 25 and 40°C in the four buffers studied. Linear fits to the data are shown as solid lines. The correlation coefficients for buffers 1 through 4 were: 5°C: 0.91, 0.93, 0.89, 0.93; 25°C: 0.99, 0.99, 0.98, 0.99; 40ºC: 0.97, 0.98, 0.97, 0.96.

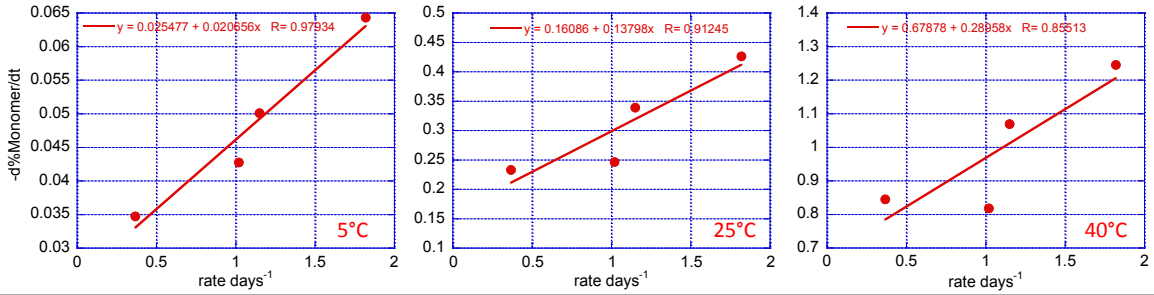

Figure 6-9. Correlation between the rate of monomer disappearance obtained by SEC at 5, 25, and 40°C, and the denaturation/aggregation rates determined by isothermal calorimetry at 60°C and 100mg/mL. The data points correspond to the four different formulation buffers.

rate is observed in buffer 4. Buffer 2 and 3 occupy intermediate positions, buffer 3 being better than buffer 2. This rank order is the same as the one observed in the isothermal calorimetry experiments. Only at 40°C, the SEC data does not provide a robust discrimination between buffers 3 and 4. Overall, there is a quantitative correlation between the rate of monomer dissapearance observed by SEC and the denaturation/aggregation rates obtained by isothermal calorimetry as shown in **Figure 6-9**. In this figure, the slopes (percent monomer vs time) calculated from the SEC data for the three temperatures studied have been plotted versus the denaturation/aggregation rates measured by the isothermal at 60°C. The correlation is excellent and characterized by correlation coefficients of 0.98, 0.91 and 0.86 at 5°C, 25°C and 40°C respectively.

Time Dependence of Denaturation/Aggregation of VRC07-523LS. The results obtained by isothermal calorimetry yield the rates of denaturation/aggregation which allow calculation of the population of denatured/aggregated antibody as a function of time for the four different formulation buffers. The results are shown in **Figure 6-10**.

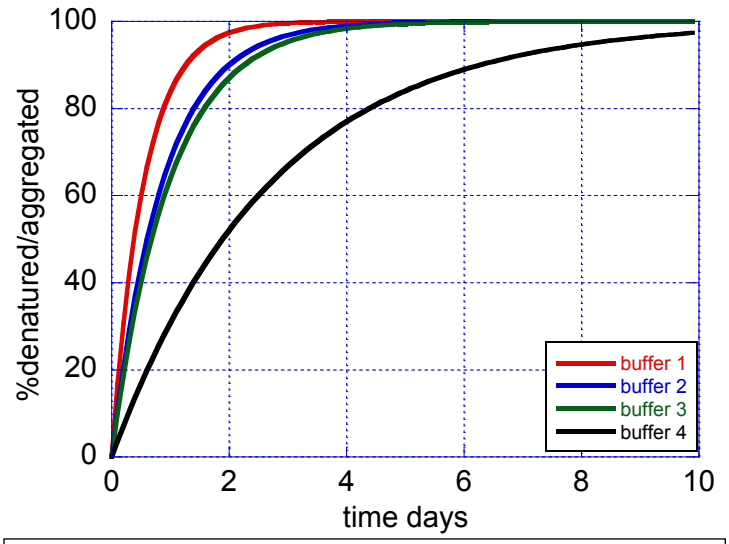

Figure 6-10. The time dependence for the formation of denatured/aggregated VRC07-523LS antibody at 60°C in the four different formulation buffers studied. The curves were calculated with the experimental rates obtained by isothermal calorimetry.

It is clear that the appearance of denatured/aggregated antibody occurs much faster in buffer 1 and much more slowly in buffer 4. In fact, at the incubation temperature of 60°C, in about two days almost all the protein is denatured/aggregated in buffer 1, whereas in buffer 4 the same level of denaturation/aggregation only occurs in more than ten days. This observation is not surprising as the essential difference between buffer 1 and buffer 4 is the addition to the latter of 5% sucrose and 2.5% sorbitol, two excipients that stabilize the native state and mitigate aggregation and are widely used in the formulation of biologics (*15-17, 69, 70*).

Temperature Dependence of Denaturation/Aggregation of VRC07-523LS . Since the combined SEC and the isothermal calorimetry experiments provide rates at four different temperatures, it was possible to perform a rigorous thermodynamic analysis in order to learn more about the temperature dependence of the long term stability of

VRCO7-523LS. For this analysis, we chose the data obtained for buffers 1 and 4 which represents the two extremes in terms of kinetic rates. In general the rates can be expressed as:

$$\ln k = -\frac{\Delta G^{\dagger}}{RT} = -\frac{\Delta H^{\dagger} - T\Delta S^{\dagger}}{RT} \qquad (7)$$

Where $\Delta G^{\dagger}$, $\Delta H^{\dagger}$ and $\Delta S^{\dagger}$ are the activations energy, enthalpy and entropy respectively. In protein stability it is well known that the enthalpy and entropy are temperature dependent due to the existence of a heat capacity difference between the denatured and native states (*22, 23, 25, 71-75*). Accordingly, the activation enthalpy and entropy can be written as:

$$\Delta H^{\dagger} = \Delta H^{\dagger}_{ref} + \Delta C_p^{\dagger}(T - T_{ref}) \qquad (8a)$$

$$\Delta S^{\dagger} = \Delta S^{\dagger}_{ref} + \Delta C_p^{\dagger}\, ln(\frac{T}{T_{ref}}) \qquad (8b)$$

Figure 6-11 shows the results of non-linear least squares fit of the combined SEC-isothermal calorimetry rate data for buffers 1 and 4 to equations 7 – 8. The data and fits have been plotted as a function of temperature rather than the inverse temperature in order to faciltate visualization. The resulting parameters at 25°C are summarized in **Table 6-2** and can be used to calculate the rates at any other temperature (equations 7 – 8). The experimental activation energies obtained from the SEC data ($\Delta G^{\dagger}_{exp}$) are very close to those obtained from the fits ($\Delta G^{\dagger}$). Also, at all temperatures the activation energy differences between buffers 1 and 4 are small and differ by 0.3 kcal/mol or less at 25°C. The data as well as the fits indicate that minor differences in activation energies have significant effects in long term stability. Most importantly is the existence of a change in the heat capacity of activation ($\Delta Cp^{\dagger}$) on the order of 1.3 kcal/K*mol. The existence of a $\Delta Cp^{\dagger}$ is responsible for the out-of-linearity of Arrhenius plots and is especially noticeable

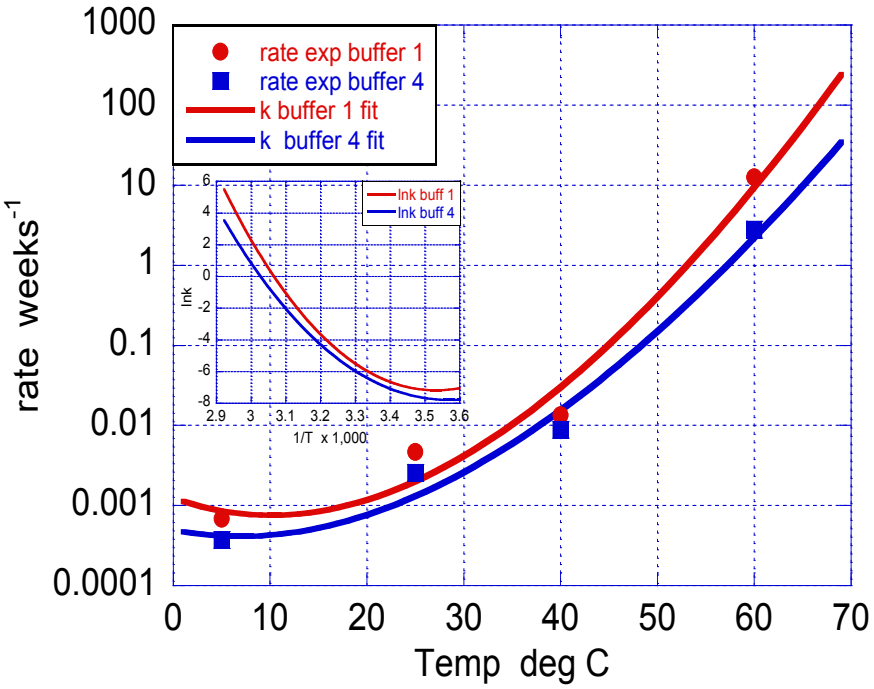

Figure 6-11. Temperature dependence of the long term stability of VRC07-523LS (*k* vs Temp) obtained by combining SEC data measured at 5, 25 and 40°C and isothermal calorimetry data obtained at 60°C. The solid lines are the results of the non-linear least squares fit of the data using equations 7 – 8. The inset shows the Arrhenius plot (lnk vs 1/T) illustrating the nonlinearity arising from the existence of a $\Delta C_p^{\dagger}$.

Table 6-2

Long Term Stability Arrhenius Parameters for VRC07-523LS at 25°C

	$\Delta G^{\dagger}$exp kcal/mol	$\Delta G^{\dagger}$ kcal/mol	$\Delta H^{\dagger}$ kcal/mol	$\Delta S^{\dagger}$ cal/K*mol	$\Delta C_p{}^{\dagger}$ kcal/K*mol
Buffer 1	3.2	3.68	22.4	62.8	1.5
Buffer 4	3.5	3.93	21.7	59.6	1.2

at low temperatures (see inset in Figure 10). This non-linearity in Arrhenius plots has been observed before (see for example (*76-78*)) and is critical for the prediction of long term stability at low temperatures from data obtained at high temperature. In fact, neglecting the non-linearity of the Arrhenius plot grossly exaggerates the expected long term stability of a monoclonal antibody as observed before (*77*). For example, at 5°C the monomer is expected to decrease to 50% in 20 - 30 years according to the SEC data and the calculated rate considering $\Delta Cp^{\dagger}$ (**Figure 6-10**).

Neglecting the $\Delta Cp^{\dagger}$ and performing a linear Arrhenius extrapolation of the rate constant from high temperature would predict a monomer decrease to 50% in hundreds of years as also observed by Drenski et al (*77*).

It is tempting to compare the activation energies obtained from the isothermal calorimetry kinetic data with the activation energies for the DSC transitions. If we extrapolate the activation energies to 70°C, we obtain values on the order of 80 kcal/mol which are about half the value for the first main transition but closer to the values obtained for the second and third transitions. If this were the case, the main culprits for aggregation at low temperatures will be those domains with the smaller

activation enthalpies, since their rate constants are not expected to decrease as fast as those with the highest activation enthalpies. In the literature and depending on the monoclonal antibody, the minor peaks have been observed either below or above the main transition and are often associated with the denaturation of the CH2 and CH3 domains (*61, 62*).

Conclusions

The aggregation profiles of monoclonal antibodies measured at 5, 25 and 40°C by size exclusion chromatography have become a standard piece of information in the evaluation of monoclonal antibody developability and formulation optimization. However, SEC experiments might take months before providing reliable results, especially at low incubation temperatures. The availability of techniques that might provide a quick and accurate ranking of different antibodies and/or formulations would greatly benefit the development of protein drugs. Here, we presented the use of isothermal calorimetry as a potential tool to evaluate the expected long term stability of monoclonal antibodies in a few days. Since isothermal calorimetry measures the kinetic rates of denaturation/aggregation of proteins below their transition temperature, it may play a valuable role in antibody selection and formulation optimization. Here we have shown that the kinetic rates of denaturation/aggregation obtained by isothermal calorimetry closely correlates with the SEC data. Also, a kinetic/thermodynamic analysis of the DSC data in conjunction with isothermal calorimetry data provides similar rankings for the formulation buffers and clues for the identification of the most likely domains to affect stability at low temperatures.

Acknowledgments

This work was supported by a grant from the National Science Foundation MCB-1157506 (EF) and by the Intramural Research Program of the Vaccine Research Center, NIAID, National Institutes of Health. We also acknowledge Jie Liu, Michael Bender, Erwin Rosales, Kandace Linkous, and Yile Li at the Vaccine Production Program for analytical support.

Chapter 7. Isothermal calorimetry of a monoclonal antibody using a conventional differential scanning calorimeter.

This chapter was published in Analytical Biochemistry (Clarkson et. al. 2018).

Abstract

It has been previously shown that isothermal calorimetry is able to provide critical information regarding the kinetics of denaturation/aggregation of monoclonal antibodies at temperatures below Tm or the onset temperature. Those measurements, however, required sophisticated specialized instrumentation. In this communication, we demonstrate that similar measurements can be performed using widely available conventional differential scanning calorimeters (DSC) when operated in isothermal scan mode. The denaturation/aggregation kinetics of the anti-HIV monoclonal antibody VRC07-523LS was previously measured by isothermal calorimetry at ten degrees below Tm. It was observed that the rates measured by isothermal calorimetry correlated quantitatively with those measured by size exclusion chromatography, thus suggesting that isothermal calorimetry can become a valuable tool for a fast prediction of the best

formulations. In this paper, similar isothermal calorimetry measurements are performed with the same antibody using a standard DSC instrument. It is shown that a readily available instrument can also provide similar kinetic information.

Introduction

Formulating a monoclonal antibody at 100mg/mL or even higher concentrations gives rise to different challenges, including maintaining the structural stability of the antibody and minimizing any tendency to aggregate over long periods of time (*13, 79*). An important criterion is the long term stability of the antibody. Unfortunately, conventional methods to rapidly predict long term stability are not always reliable. Often, results obtained from accelerated conditions do not correlate with aggregation pattern observed by size exclusion chromatography (SEC) obtained after long incubation times (*80, 81*).

Previously, we utilized isothermal calorimetry as a novel technique to measure the kinetics of denaturation/aggregation of a monoclonal antibody (VRC07-523LS), and compare the results with those obtained by size exclusion chromatography (SEC) (*82*). Isothermal calorimetry is able to measure the rate of heat production or absorption associated with the denaturation and aggregation of the antibody at a given temperature over days or weeks. However, in that paper we employed a sophisticated instrument (TAM IV, TA Instruments, New Castle, DE, USA) with the capability of measuring up to 48 samples simultaneously. In this paper, the kinetics of denaturation/aggregation of the monoclonal antibody VRC07-523LS was measured by isothermal calorimetry using a widely available capillary DSC instrument operating in the isothermal scan mode. It is

shown, that for measuring single samples this instrument provides a readily accessible alternative to more sophisticated instruments.

Materials and Methods

Proteins and Reagents: VRC07-523LS was obtained from the NIH Vaccine Research Center (VRC) in Gaithersburg, MD as described earlier (*82*). Two different formulation buffers were chosen for these studies: buffer 1 (50 mM histidine, 100 mM NaCl, pH 6.8) and buffer 4 (50 mM histidine, 50 mM NaCl, 5% w/v sucrose, 2.5% w/v sorbitol, pH 6.8). Chemicals for buffer preparation were purchased from multiple vendors: L-Histidine (98%, CAS 71-00-1) from Acros Organics (New Jersey, USA), NaCl (Certified ACS/Crystalline, CAS 7647-14-5) from Fisher Scientific (Fair Lawn, NJ, USA), and sucrose (minimum 99.5%, CAS 57-50-1) and D-sorbitol (minimum 98%, CAS 50-70-4) from Sigma-Aldrich (St. Louis, MO, USA).

Differential Scanning Calorimetry: Isothermal calorimetry experiments were performed using a capillary cell VP-DSC microcalorimeter from MicroCal/Malvern Instruments (Northampton, MA, USA). The total volume of the calorimeter cell is 0.5mL. Experiments were performed as described in the Results and Discussion section. Due to the high protein concentrations used in long term stability studies, the contents of the sample cell at the end of each experiment were a solid paste of precipitated protein. The cell was cleaned by successive cycles of removing any excess liquid, adding enough 70% nitric acid to fill the cell, and heating the instrument to 80°C until all precipitated protein was dissolved as judged by the clarity of the liquid removed from the cell after each heating cycle. Data collection and processing of raw data were performed using the software provided with the instrument. Data analysis was

performed using equations described previously (*82, 83*) and implemented in the DataFit software package (Oakdale Engineering, Oakdale, PA, USA).

Results and Discussion

Isothermal Calorimetry Using Conventional DSC. Isothermal calorimetry experiments were performed using the isothermal scan mode which is provided in the instrument software. The experiments reported here were performed by using the "constant temperature" setting and no instrument feedback. In our experiments, the "constant temperature" setting option was selected instead of the alternative "low noise" option, as the instrument did not maintain a precisely constant temperature using the low noise option. Using the constant temperature option, allowed us to perform experiments at closely spaced temperatures (e.g. 1°C). It must be noted that at temperatures close to the onset transition temperature at which most isothermal calorimetry experiments are performed (60 – 62°C for VRC07), the denaturation/aggregation rates change significantly with temperature and that a precise temperature control must be maintained. Changing the feedback to medium did not have a significant effect probably due to the fact that these denaturation/aggregation processes are very slow (hours to days).

Protein solutions of ~50 mg/mL were dialyzed overnight against the desired buffer, diluted to the experimental concentration of ~50 mg/mL and thoroughly degassed. Lower protein concentrations were tried but the instrument was not able to provide a significant and reproducible signal below 50 mg/mL for this antibody. Since monoclonal antibody formulations usually require 100mg/mL or more, this requirement

is not of a particular concern and allows measurements at the formulation concentration.

Experiments were started by loading buffer into the reference and sample cells. The instrument was heated to the experimental temperature (e.g. 60°C) and held at that temperature for 5 minutes. This step is the equivalent to a buffer-buffer scan in a standard DSC experiment. The instrument was then cooled to 20°C and the buffer in the sample cell was replaced with protein. Next, the instrument was quickly (~30 minutes) heated to the experimental temperature (e.g. 60°C). Once the experimental temperature is reached, it is held constant and the differential power (DP) between the sample and reference cells is recorded as a function of time. Experiments were run until the differential power stabilized to a constant value. The average signal for the final ~6 hours of the experiment after a constant signal was achieved was considered a baseline and subtracted from the rest of the data. After baseline subtraction, the differential signal was normalized per mole of protein and expressed as kcal/day/mol.

Denaturation/Aggregation of VRC07-523LS at 61°C. The denaturation/aggregation

kinetics of VRC07-523LS was measured in buffer 1 and 4 at 61°C, which is about nine degrees below T_m (*82*). The experiments were performed in the capillary VP-DSC as described above. **Figure 7-1** shows the results of the experiments (normalized heat flow versus time). It is clear that the experiments are able to immediately identify the best formulation. The rate of denaturation/aggregation for buffer 1 at 61°C is 3.07 ± 0.014 days^{-1} (k^{-1} = 0.32 days) whereas the rate for buffer 4 is 0.715 ± 0.016 days^{-1} (k^{-1} = 1.4 days). For both buffers, the area under the curve which corresponds to the total heat of denaturation/aggregation was the same, 610 kcal/mol. Since the reaction in buffer 1 occurs much faster, the amplitude of the signal is much larger. For buffer 4, the same amount of heat is spread over a longer time and therefore the amplitude is smaller. The rates as well as the heats of denaturation/aggregation are similar to those obtained with the TAM IV (*82*). As expected, the rates at 61°C are somewhat faster than those measured at 60°C (k = 0.51 days^{-1} and k = 1.9 days^{-1} for buffer 4 and 1 respectively). For the experiments presented in this work, the signal amplitude was undistinguishable from the baseline for processes taking more than two to three days. The signal

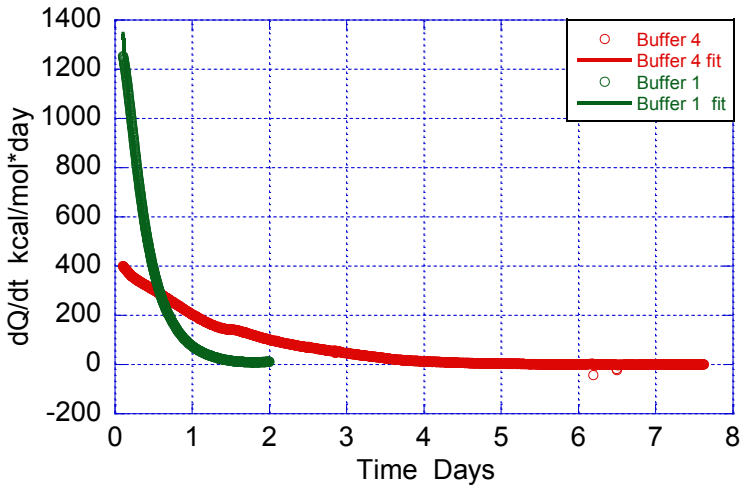

Figure 7-1. Heat flow (dQ/dt) (experimental data and fit) recorded as a function of time for VRC07-523LS at 61°C in buffer 1 (green) and buffer 4 (red). The experiments were performed at a protein concentration of 50 mg/mL in a volume of 0.518mL. The curves in the graph were obtained after subtraction of the final baseline followed by normalization by the amount of protein. A positive heat flow corresponds to an endothermic process.

amplitude can be improved either by increasing the antibody concentration or by increasing the temperature. For VRC07- 523LS in buffer 4 a reliable signal could not be obtained at temperatures lower than 61°C using a 50 mg/mL protein concentration. The strong effect of temperature is illustrated in **Figure 7-2** for VRC07- 523LS in buffer 1. At 60°C the rate of denaturation aggregation is 1.26 days^{-1} (k^{-1} = 0.79 days) compared to the value of 3.07 days-1 (k^{-1} = 0.32 days) measured at 61°C.

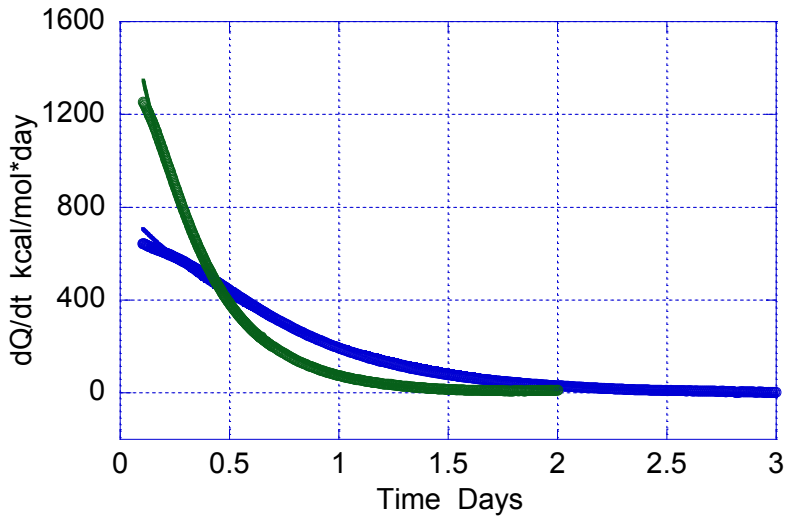

Figure 7-2. Heat flow (dQ/dt) (experimental data and fit) recorded as a function of time for VRC07-523LS at 60°C (blue) and 61°C (green) in buffer 1. The experiments were performed at a protein concentration of 50 mg/mL in a volume of 0.518mL.

Conclusion

Isothermal calorimetry provides an orthogonal, fast alternative to conventional methods for predicting long term stability of biologics. Since sophisticated isothermal calorimeters are not available in most biophysical laboratories, a readily available alternative is the use of conventional DSC instruments in the isothermal scan mode. This approach can be used to evaluate the validity of isothermal calorimetry data in the prediction of long term stability of biologics.

Acknowledgments: This work was supported by a grant from the National Science Foundation MCB-1157506 (EF). We also thank Dr. Arne Schon for many helpful discussions.

Chapter 8. Conclusions

It is important to note that the intrinsic conformational stability of proteins in solution is perhaps the most important factor in determining their aggregation propensity, but there are other factors which can lead to protein aggregation or degradation before patient administration. During post-production handling of protein during shipping or storage, or during administration, numerous events may stress the protein, only some of which can be mitigated by increased conformational stability through the addition of excipients. Most of these stresses are caused by unintentional mishandling on the part of the patient or in some cases the medical staff administering the drug, or can even be an unavoidable part of routine handling during production and transport. While patient self-administration is a highly desirable route for patient compliance and ease of treatment, it also necessitates formulations that can protect against these stresses to an even higher degree than normal. The different factors that can effect drug stability during the period of time between its production and patient administration can generally be divided into three categories: mechanical stress (including associated contact with interfaces), temperature extremes, and light exposure (*84*). The effects of temperature extremes and freeze-thaw cycles are usually tested for and addressed during formulation design and countered by the addition of stabilizing

excipients as discussed previously (*84*). Light exposure often occurs during the transport of IV bags or while warming up certain drugs for injection and can cause photodegradation of proteins and aggregation (*84*). This exposure to harmful wavelengths of light is combated by secondary packaging to block light exposure, although this only guarantees protection from light during transport and storage, but not once the drug is in the hands of patients or hospital staff. Mechanical stress can occur accidentally or through routine handling from things like dropping of protein vials or aspiration of formulations in syringes and combined with contact with various interfaces (liquid-air, liquid-solid, etc.) during mixing or administration can cause conformational change and aggregation of the protein (*84*). Various nonionic surfactants, like polysorbates, are generally added to formulations to prevent adsorption or other interactions with surfaces by minimizing the interaction between protein and any interfaces (*84*). In this way, nonionic surfactants do not increase the stability of the protein itself, but rather prevent undesirable interactions with interfaces in order to decrease protein aggregation and increase long-term stability during transport, storage and administration. And while this is clearly necessary, especially with drugs that have been shown to have adsorption problems or a particular sensitivity to agitation, measuring the effect of these excipients is not always straightforward. Traditional techniques that measure protein stability like DSC, ICD, or even isothermal calorimetry, reliably capture the effect of stabilizing or solubilizing excipients, but don't capture the effect of limiting undesirable interactions with interfaces very well in a timely way. Clearly a traditional long-term stability study using SEC at different time points could conceivably capture the effect of surfactants on aggregation during long-term storage,

and stirring or agitation could be added to the experimental design as well. But a better understanding of the effects of real-world handling of drug formulations is clearly necessary in order to improve formulation design. Both the extent to which the stresses mentioned above impact protein aggregation and degradation, as well as how much the efficacy and safety of the drugs are effected, are crucial parts of that understanding.

Biologics are a crucial part of effective treatment of patient symptoms and disease and are rapidly becoming a large focus of the pharmaceutical industry. While more traditional small molecule drugs are very cheap and easy to make, biologics are generally significantly more potent and specific. But biologics are extremely complicated to manufacture, characterize, and store, as they are large complex molecules that are very sensitive to environmental and storage conditions. They are prone to degradation or aggregation, which not only decreases drug potency, but can also cause painful drug administration or severe immune responses in patients.

I have briefly detailed the most commonly used techniques to measure aggregation in drug formulations in order to clarify their utility and short comings in the formulation development process. In short, these techniques do a fair job of characterizing the stability of biologics in formulation, but provide little predictive power, leading any investigation into the effect of storage conditions on drug stability to necessitate long incubation times. To address this problem, I have developed isothermal calorimetry for use with high concentration biologic formulations. Using this technique, the rates of unfolding and aggregation can be measured for proteins under formulation conditions at temperatures well below T_m and compared between conditions to select the best formulation. In some situations where very sensitive measurements

are called for, such as proteins that are very stable in formulation and therefore only minimally aggregate, expensive specialized instrumentation may be required instead of a more readily available conventional DSC run in isothermal mode. Also, while data can often be fit by a simple single exponential decay (as presented in this work) to extract unfolding or aggregation rate constants, more complicated aggregation pathways can lead to isothermal calorimetry data that is difficult to fit in order to extract useful information, necessitating the use of other techniques to assist in understanding the experimental data. Finally, isothermal calorimetry is a bulk measurement technique, so the interpretation of data for formulations with multiple mAbs in them may be complicated to untangle. But given these minor constraints, isothermal calorimetry is an exceedingly useful technique for assessing protein stability in formulation. Unlike other techniques which either hold no predictive power by design (e.g. SEC), or measure quantities that may correlate poorly with long-term stability (e.g. ICD), isothermal calorimetry measures unfolding and aggregation rates which correlate closely with results from long-term stability studies done with SEC. Furthermore, isothermal calorimetry experiments can be conducted with buffer conditions exactly mimicking those in formulation rather than being limited to only low protein concentrations or certain buffers. In fact, the signal to noise ratio of isothermal calorimetry data improves with increased protein concentration, making it ideal for use with high concentration formulations.

Protein stability and aggregation is a complicated balancing act of interactions between the protein and solvent, the protein and other proteins, numerous types of forces like the hydrophobic effect and ionic bonds, the actual physical conditions

present, and numerous others. This confluence of factors makes a complete and thorough understanding of these processes complicated, and any new pieces of information can unlock a further understanding. The ability to measure the rate of unfolding and/or aggregation under the exact physical and chemical conditions present in formulation is crucial to a complete understanding of proteins in formulation, particularly because its interpretation is so straightforward. Comparing the aggregation rate to other well established measurements like ΔG or more difficult to interpret values can also assist in a deeper understanding of the way different parameters effect the aggregation behavior of proteins.

Techniques like AUC and chemical denaturation have been irreplaceable in forming our current knowledge of protein aggregation, and continue to be an important part of formulation development and scientific research, particularly due to the complicated aggregation pathways of many large molecules involving partially denatured states. But in terms of predicting the shelf life of biologics and better understanding their long-term aggregation kinetics, isothermal calorimetry fills an empty niche. It can obtain useful quantitative information on proteins at the high concentrations used in formulations (~100 mg/mL) and with relatively mild denaturing conditions, and can provide useful information with less necessary extrapolation than techniques which use lower protein concentrations or high temperatures or denaturant concentrations. Isothermal calorimetry does a very good job at predicting the results obtained using much more time consuming techniques like SEC, so the adoption of isothermal calorimetry as part of formulation development could significantly decrease

the required time for shelf-life prediction, thereby decreasing the time required to get lifesaving drugs in the hands of patients.

References

1. Kasimova, M. R., Milstein, S. J., and Freire, E. (1998) The conformational equilibrium of human growth hormone, *J Mol Biol 277*, 409-418.
2. Rosati, S., Yang, Y., Barendregt, A., and Heck, A. J. (2014) Detailed mass analysis of structural heterogeneity in monoclonal antibodies using native mass spectrometry, *Nat Protoc 9*, 967-976.
3. Todd, M. J., Semo, N., and Freire, E. (1998) The structural stability of the HIV-1 protease, *J Mol Biol 283*, 475-488.
4. Jones, A. W. (2011) Early drug discovery and the rise of pharmaceutical chemistry, *Drug Test Anal 3*, 337-344.
5. Schwerin, A., Stoff, H., and Wahrig, B. (2013) *Biologics. A History of Agents Made from Living Organisms in the Twentieth Century*.
6. Lybecker, K. (2016) The Biologics Revolution in the Production of Drugs, Fraser Institute.
7. Sekhon, B., and Saluja, V. (2011) *Biosimilars: An overview*, Vol. 1.
8. Stanczyk, J., Ospelt, C., and Gay, S. (2008) Is there a future for small molecule drugs in the treatment of rheumatic diseases?, *Curr Opin Rheumatol 20*, 257-262.
9. EvaluatePharma®. (2016) World Preview 2016, Outlook to 2022, 9 ed.
10. Skalko-Basnet, N. (2014) Biologics: the role of delivery systems in improved therapy, *Biologics 8*, 107-114.
11. Haller, M. F. (2007) Converting Intravenous Dosing to Subcutaneous Dosing With Recombinant Human Hyaluronidase, *Pharmaceutical Technology 31*.
12. Wang, W. (2015) Advanced protein formulations, *Protein Sci 24*, 1031-1039.

13. Shire, S. J., Shahrokh, Z., and Liu, J. (2004) Challenges in the development of high protein concentration formulations, *J Pharm Sci 93*, 1390-1402.

14. Connolly, B. D., Petry, C., Yadav, S., Demeule, B., Ciaccio, N., Moore, J. M., Shire, S. J., and Gokarn, Y. R. (2012) Weak interactions govern the viscosity of concentrated antibody solutions: high-throughput analysis using the diffusion interaction parameter, *Biophys J 103*, 69-78.

15. Kamerzell, T. J., Esfandiary, R., Joshi, S. B., Middaugh, C. R., and Volkin, D. B. (2011) Protein-excipient interactions: mechanisms and biophysical characterization applied to protein formulation development, *Adv Drug Deliv Rev 63*, 1118-1159.

16. Street, T. O., Bolen, D. W., and Rose, G. D. (2006) A molecular mechanism for osmolyte-induced protein stability, *Proc Natl Acad Sci U S A 103*, 13997-14002.

17. Bolen, D. W. (2001) Protein stabilization by naturally occurring osmolytes, *Methods Mol Biol 168*, 17-36.

18. Hong, P., Koza, S., and Bouvier, E. S. (2012) Size-Exclusion Chromatography for the Analysis of Protein Biotherapeutics and their Aggregates, *J Liq Chromatogr Relat Technol 35*, 2923-2950.

19. Berkowitz, S. A. (2006) Role of analytical ultracentrifugation in assessing the aggregation of protein biopharmaceuticals, *AAPS J 8*, E590-605.

20. Murphy, R. M. (1997) Static and dynamic light scattering of biological macromolecules: what can we learn?, *Curr Opin Biotechnol 8*, 25-30.

21. den Engelsman, J., Garidel, P., Smulders, R., Koll, H., Smith, B., Bassarab, S., Seidl, A., Hainzl, O., and Jiskoot, W. (2011) Strategies for the assessment of

protein aggregates in pharmaceutical biotech product development, *Pharm Res 28*, 920-933.

22. Freire, E. (1995) Differential scanning calorimetry, *Methods Mol Biol 40*, 191-218.
23. Freire, E., and Biltonen, R. L. (1978) Statistical mechanical deconvolution of thermal transitions in macromolecules. I. Theory and application to homogeneous systems, *Biopolymers 17*, 463-479.
24. Privalov, P. L., and Khechinashvili, N. N. (1974) A Thermodynamic Approach to the Problem of Stabilization of Globular Protein Structure: A Calorimetric Study, *Journal of Molecular Biology 86*, 665-684.
25. Privalov, P. L., and Potekhin, S. A. (1986) Scanning microcalorimetry in studying temperature-induced changes in proteins, *Methods Enzymol 131*, 4-51.
26. Borzova, V. A., Markossian, K. A., Chebotareva, N. A., Kleymenov, S. Y., Poliansky, N. B., Muranov, K. O., Stein-Margolina, V. A., Shubin, V. V., Markov, D. I., and Kurganov, B. I. (2016) Kinetics of Thermal Denaturation and Aggregation of Bovine Serum Albumin, *PLoS One 11*, e0153495.
27. Greene, R. F., Jr., and Pace, C. N. (1974) Urea and guanidine hydrochloride denaturation of ribonuclease, lysozyme, alpha-chymotrypsin, and beta-lactoglobulin, *J Biol Chem 249*, 5388-5393.
28. Pace, C. N., Laurents, D. V., and Erickson, R. E. (1992) Urea denaturation of barnase: pH dependence and characterization of the unfolded state, *Biochemistry 31*, 2728-2734.

29. Freire, E., Schon, A., Hutchins, B. M., and Brown, R. K. (2013) Chemical denaturation as a tool in the formulation optimization of biologics, *Drug Discovery Today 18*, 1007-1013.

30. Bolen, D. W., and Santoro, M. M. (1988) Unfolding free energy changes determined by the linear extrapolation method. 2. Incorporation of dGn-u values in a thermodynamic cycle, *Biochemistry 27*, 8069-8074.

31. Santoro, M. M., and Bolen, D. W. (1988) Unfolding free energy changes determined by the linear extrapolation method. 1. Unfolding of phenylmethanesulfonyl.alpha.chymotrypsin using different denaturants, *Biochemistry 27*, 8063-8068.

32. Rudicell, R. S., Kwon, Y. D., Ko, S. Y., Pegu, A., Louder, M. K., Georgiev, I. S., Wu, X., Zhu, J., Boyington, J. C., Chen, X., Shi, W., Yang, Z. Y., Doria-Rose, N. A., McKee, K., O'Dell, S., Schmidt, S. D., Chuang, G. Y., Druz, A., Soto, C., Yang, Y., Zhang, B., Zhou, T., Todd, J. P., Lloyd, K. E., Eudailey, J., Roberts, K. E., Donald, B. R., Bailer, R. T., Ledgerwood, J., Mullikin, J. C., Shapiro, L., Koup, R. A., Graham, B. S., Nason, M. C., Connors, M., Haynes, B. F., Rao, S. S., Roederer, M., Kwong, P. D., Mascola, J. R., and Nabel, G. J. (2014) Enhanced potency of a broadly neutralizing HIV-1 antibody in vitro improves protection against lentiviral infection in vivo, *J Virol 88*, 12669-12682.

33. Andrews, J. M., and Roberts, C. J. (2007) A Lumry-Eyring nucleated polymerization model of protein aggregation kinetics: 1. Aggregation with pre-equilibrated unfolding, *J Phys Chem B 111*, 7897-7913.

34. Lumry, R., and Eyring, H. (1954) Conformation Changes of Proteins, *The Journal of Physical Chemistry 58*, 110-120.

35. Clarkson, B. R., Schon, A., and Freire, E. (2016) Conformational stability and self-association equilibrium in biologics, *Drug Discov Today 21*, 342-347.

36. Ericsson, U. B., Hallberg, B. M., DeTitta, G. T., Dekker, N., and Nordlund, P. (2006) Thermofuor-based high-throughput stability optimization of proteins for structural studies, *Anal. Biochem 357*, 289-298.

37. Vedadi, M., Niesen, F. H., Allali-HAssani, A., Fedorov, O. Y., Finerty Jr, P. J., Wasney, G. A., Yeung, R., Arrowsmith, C., Ball, L. J., Berglund, H., Hui, R., Marsden, B. D., Nordlund, P., Sundstrom, M., Weigelt, J., and Edwards, A. M. (2006) Chemical screening methods to identify ligands that promote protein stability, protein crystallization and structure determination, *Proc. Natl. Acad. Sci. (USA) 103*, 15835-15840.

38. Capelle, M. A. H., Gurny, R., and Arvinte, T. (2007) High throughput screening of protein formulation stability: Practical considerations, *Eurpean J. Pharmaceutics and Biopharmaceutics 65*, 131-148.

39. Senisterra, G. A., and Finerty Jr., P. J. (2009) High throughput methods of assessing protein stability and aggregation, *Mol. BioSyst. 5*, 217-223.

40. Privalov, P. L. (1979) Stability of Proteins: Small Globular Proteins, *Advances in Protein Chemistry 33*, 167-239.

41. Privalov, P. L. (1982) Stability of Proteins: Proteins Which Do Not Present a Single Cooperative System, *Advances in Protein Chemistry 35*, 1-104.

42. Brandts, J. F., Oliveira, R. J., and Westort, C. (1970) Thermodynamics of protein denaturation. Effect of pressure on the denaturation of ribonuclease A, *Biochemistry 9*, 1038-1047.

43. Privalov, G., Kavina, V., Freire, E., and Privalov, P. L. (1995) Precise Scanning Calorimeter for Studying Thermal Properties of Biological Macromolecules in Dilute Solution, *Anal. Biochem. 232*, 79-85.

44. Greene, R. F., Jr., and Pace, C. N. (1974) Urea and guanidine hydrochloride denaturation of ribonuclease, lysozyme, alpha-chymotrypsin, and beta-lactoglobulin, *J. Biol. Chem. 249*, 5388-5393.

45. Pace, C. N., Laurents, D. V., and Erickson, R. E. (1992) Urea denaturation of barnase: pH dependence and characterization of the unfolded state, *Biochemistry 31*, 2728-2734.

46. Myers, J. K., Pace, C. N., and Scholtz, J. M. (1995) Denaturant m values and heat capacity changes: Relation to changes in accessible surface area of protein unfolding, *Prot. Science 4*, 2138-2148.

47. Schon, A., Clarkson, B. R., Siles, R., Ross, P., Brown, R. K., and Freire, E. (2015) Denatured State Aggregation Parameters Derived from Concentration Dependence of Protein Stability, *Analytical Biochemistry In Press*.

48. Messersmith, W. A., and Ahnen, D. J. (2008) Targeting EGFR in colorectal cancer, *N Engl J Med 359*, 1834-1836.

49. Wu, X., Yang, Z. Y., Li, Y., Hogerkorp, C. M., Schief, W. R., Seaman, M. S., Zhou, T., Schmidt, S. D., Wu, L., Xu, L., Longo, N. S., McKee, K., O'Dell, S., Louder, M. K., Wycuff, D. L., Feng, Y., Nason, M., Doria-Rose, N., Connors, M.,

Kwong, P. D., Roederer, M., Wyatt, R. T., Nabel, G. J., and Mascola, J. R. (2010) Rational design of envelope identifies broadly neutralizing human monoclonal antibodies to HIV-1, *Science 329*, 856-861.

50. Wang, W., Singh, S., Zeng, D. L., King, K., and Nema, S. (2007) Antibody structure, instability, and formulation, *Journal of Pharmaceutical Sciences 96*, 1-26.

51. Chaudhuri, R., Cheng, Y., Middaugh, C. R., and Volkin, D. B. (2014) High-throughput biophysical analysis of protein therapeutics to examine interrelationships between aggregate formation and conformational stability, *AAPS J 16*, 48-64.

52. Li, Y., Mach, H., and Blue, J. T. (2011) High throughput formulation screening for global aggregation behaviors of three monoclonal antibodies, *J Pharm Sci 100*, 2120-2135.

53. Cordes, A. A., Carpenter, J. F., and Randolph, T. W. (2012) Accelerated stability studies of abatacept formulations: comparison of freeze-thawing- and agitation-induced stresses, *J Pharm Sci 101*, 2307-2315.

54. Hawe, A., Wiggenhorn, M., van de Weert, M., Garbe, J. H., Mahler, H. C., and Jiskoot, W. (2012) Forced degradation of therapeutic proteins, *J Pharm Sci 101*, 895-913.

55. Wang, T., Kumru, O. S., Yi, L., Wang, Y. J., Zhang, J., Kim, J. H., Joshi, S. B., Middaugh, C. R., and Volkin, D. B. (2013) Effect of ionic strength and pH on the physical and chemical stability of a monoclonal antibody antigen-binding fragment, *J Pharm Sci 102*, 2520-2537.

56. Weiss, W. F. t., Young, T. M., and Roberts, C. J. (2009) Principles, approaches, and challenges for predicting protein aggregation rates and shelf life, *J Pharm Sci 98*, 1246-1277.

57. Freire, E., van Osdol, W. W., Mayorga, O. L., and Sanchez-Ruiz, J. M. (1990) Calorimetrically determined dynamics of complex unfolding transitions in proteins, *Annu Rev Biophys Biophys Chem 19*, 159-188.

58. Sanchez-Ruiz, J. M., Lopez-Lacomba, J. L., Cortijo, M., and Mateo, P. L. (1988) Differential scanning calorimetry of the irreversible thermal denaturation of thermolysin, *Biochemistry 27*, 1648-1652.

59. Schön, A., Clarkson, B. R., Jaime, M., and Freire, E. (2017) Temperature stability of proteins: Analysis of irreversible denaturation using isothermal calorimetry, *Proteins: Structure, Function, and Bioinformatics 85*, 2009-2016.

60. Schön, A., and Freire, E. (2017) Analysis of Long Term Stability of Biologics by Isothermal Calorimetry., TA Instruments literature.

61. Ionescu, R. M., Vlasak, J., Price, C., and Kirchmeier, M. (2008) Contribution of variable domains to the stability of humanized IgG1 monoclonal antibodies, *J Pharm Sci 97*, 1414-1426.

62. Wen, J., Jiang, Y., and Nahri, L. (2008) *Effect of Carbohydrate on Thermal Stability of Antibodies*, Vol. 11.

63. Wen, J., Arthur, K., Chemmalil, L., Muzammil, S., Gabrielson, J., and Jiang, Y. (2012) Applications of differential scanning calorimetry for thermal stability analysis of proteins: qualification of DSC, *J Pharm Sci 101*, 955-964.

64. Ibarra-Molero, B., and Sanchez-Ruiz, J. M. (1997) Are there equilibrium intermediate states in the urea-induced unfolding of hen egg-white lysozyme?, *Biochemistry 36*, 9616-9624.

65. Kurganov, B. I., Lyubarev, A. E., Sanchez-Ruiz, J. M., and Shnyrov, V. L. (1997) Analysis of differential scanning calorimetry data for proteins. Criteria of validity of one-step mechanism of irreversible protein denaturation, *Biophys Chem 69*, 125-135.

66. Sanchez-Ruiz, J. M. (1992) Theoretical analysis of Lumry-Eyring models in differential scanning calorimetry, *Biophys J 61*, 921-935.

67. Lazar, K. L., Patapoff, T. W., and Sharma, V. K. (2010) Cold denaturation of monoclonal antibodies, *MAbs 2*, 42-52.

68. Robertson, A. D., and Murphy, K. P. (1997) Protein Structure and the Energetics of Protein Stability, *Chem Rev 97*, 1251-1268.

69. Ohtake, S., Kita, Y., and Arakawa, T. (2011) Interactions of formulation excipients with proteins in solution and in the dried state, *Adv Drug Deliv Rev 63*, 1053-1073.

70. Warne, N. W. (2011) Development of high concentration protein biopharmaceuticals: the use of platform approaches in formulation development, *Eur J Pharm Biopharm 78*, 208-212.

71. Makhatadze, G. I., and Privalov, P. L. (1990) Heat capacity of proteins. I. Partial molar heat capacity of individual amino acid residues in aqueous solution: hydration effect, *J Mol Biol 213*, 375-384.

72. Murphy, K. P., and Freire, E. (1992) Thermodynamics of structural stability and cooperative folding behavior in proteins, *Adv Protein Chem 43*, 313-361.

73. Murphy, K. P., and Gill, S. J. (1991) Solid model compounds and the thermodynamics of protein unfolding, *J Mol Biol 222*, 699-709.

74. Privalov, P. L., and Makhatadze, G. I. (1990) Heat capacity of proteins. II. Partial molar heat capacity of the unfolded polypeptide chain of proteins: protein unfolding effects, *J Mol Biol 213*, 385-391.

75. Privalov, P. L., Tiktopulo, E. I., Venyaminov, S., Griko Yu, V., Makhatadze, G. I., and Khechinashvili, N. N. (1989) Heat capacity and conformation of proteins in the denatured state, *J Mol Biol 205*, 737-750.

76. Brader, M. L., Estey, T., Bai, S., Alston, R. W., Lucas, K. K., Lantz, S., Landsman, P., and Maloney, K. M. (2015) Examination of thermal unfolding and aggregation profiles of a series of developable therapeutic monoclonal antibodies, *Mol Pharm 12*, 1005-1017.

77. Drenski, M. F., Brader, M. L., Alston, R. W., and Reed, W. F. (2013) Monitoring protein aggregation kinetics with simultaneous multiple sample light scattering, *Anal Biochem 437*, 185-197.

78. Wang, W., and Roberts, C. J. (2013) Non-Arrhenius protein aggregation, *AAPS J 15*, 840-851.

79. Wang, W., Singh, S., Zeng, D. L., King, K., and Nema, S. (2007) Antibody structure, instability, and formulation, *J Pharm Sci 96*, 1-26.

80. Shi, S., Semple, A., Cheung, J., and Shameem, M. (2013) DSF method optimization and its application in predicting protein thermal aggregation kinetics, *J Pharm Sci 102*, 2471-2483.

81. Thiagarajan, G., Semple, A., James, J. K., Cheung, J. K., and Shameem, M. (2016) A comparison of biophysical characterization techniques in predicting monoclonal antibody stability, *MAbs 8*, 1088-1097.

82. Clarkson, B. R., Chaudhuri, R., Schon, A., Cooper, J. W., Kueltzo, L., and Freire, E. (2018) Long term stability of a HIV-1 neutralizing monoclonal antibody using isothermal calorimetry, *Anal Biochem 554*, 61-69.

83. Schon, A., Clarkson, B. R., Jaime, M., and Freire, E. (2017) Temperature stability of proteins: Analysis of irreversible denaturation using isothermal calorimetry, *Proteins 85*, 2009-2016.

84. Nejadnik, M. R., Randolph, T. W., Volkin, D. B., Schoneich, C., Carpenter, J. F., Crommelin, D. J. A., and Jiskoot, W. (2018) Postproduction Handling and Administration of Protein Pharmaceuticals and Potential Instability Issues, *J Pharm Sci 107*, 2013-2019.

Curriculum Vitae

BENJAMIN R. CLARKSON

Born May 7th, 1992 in Beverly, MA

Johns Hopkins University | 617-842-3427 | bnclarkson@gmail.com

EDUCATION

Johns Hopkins University Cellular, Molecular, and Developmental Biology and Biophysics Doctoral Graduate Program (August 2014 – present). Expected graduation: January 2019. Ernesto Freire Laboratory.

Davidson College, BS in Biology, GPA = 3.33 (August 2010 – May 2014)

Semester in Berlin, Germany (Aug – Dec., 2012)

GRADUATE RESEARCH

Biochemical and Biophysical Research (May 2015-present) Johns Hopkins University

Mentor: Ernesto Freire

Studied the stability of monoclonal antibodies in formulation using a variety of both common and novel approaches. Extensively utilized DSC and chemical denaturation to measure stability and aggregation propensity under different conditions. Also developed novel use of isothermal calorimetry to measure rates of denaturation and aggregation at formulation protein concentrations. Rank order of different formulations obtained using this technique matched exactly with the ranking from traditional SEC experiments to determine long-term stability.

UNDERGRADUATE RESEARCH

Synthetic Biology Research (Fall 2013) Davidson College

Mentors: Drs. A. Malcolm Campbell and Laurie J. Heyer

Engineered yeast cells to optimize production of desirable metabolites.

Synthetic Biology and Bioenergy Research (Summer 2013) J. Craig Venter Institute

Mentors: Drs. Isaac T. Yonemoto and Philip D. Weyman

Engineered [NiFe] hydrogenase to improve hydrogen production.

Synthetic Biology Research (Summer, 2012) Davidson College

Mentors: Drs. A. Malcolm Campbell and Laurie J. Heyer

Designed and tested pH-sensitive promoters as part of collaborative research effort with biologists, computer scientists, and mathematicians.

Synthetic Biology Independent Study (Spring Semester, 2012) Davidson College

Mentors: Drs. A. Malcolm Campbell and Laurie J. Heyer

Developed new research project in cellular network control.

Cell Biology Independent Study (Spring Semester, 2011) Davidson College

Dr. Jennifer Round

Measured Heat Shock Protein 70 (HSP-70) inhibition on flagellar regeneration.

RESEARCH SKILLS

Laboratory Skills: PCR, primer design, ligation, transformation, gel electrophoresis and purification, MiniPrep, glycerol stock preparation, measuring fluorescence and luminescence in *E. coli*, microscope manipulation and usage, deflagellation and regeneration, electroporation, Gibson Assembly, Golden Gate Assembly, gas chromatography, immunostaining, confocal microscopy, chemical denaturation, differential scanning calorimetry, protein fluorescence, light scattering, size exclusion chromatography, isothermal calorimetry

Computer Skills: python programming, ApE DNA software, BLAST, Genome Browser, Wiki editing, Microscope Image Capture Software (ImageJ), CLC Genomics Workbench, Microsoft Office, data fitting using DataFit, Mathematica, KaleidaGraph

LEADERSHIP AND ORGANIZATIONAL EXPERIENCE

- One of two student representatives for graduate class who facilitated student communication with professors and organized and implemented recruitment weekend for graduate prospective graduate students.
- Organized the Christian B. Anfinsen lecture series, an entirely student run endeavor, which invited prominent scientists to visit campus to meet with students and give a lecture on their research.
- Teaching assistant for undergraduate lab classes in biochemistry and cell biology. Responsibilities included setting up and running lab classes and grading weekly assignments and exams.
- Lead teaching assistant for graduate course in biophysical chemistry. Responsibilities included running computational labs related to lecture material, grading weekly assignments and labs, running exam review sessions, and tutoring students.

PUBLICATIONS

Clarkson BR, Freire, E. Isothermal calorimetry of a monoclonal antibody using a conventional differential scanning calorimeter. Analytical Biochemistry. 2018; 558:50-52.

Clarkson BR, Chaudhuri R, Schön A, Cooper, JW, Kueltzo L, Freire E. Long Term Stability of a HIV-1 Neutralizing Monoclonal Antibody Using Isothermal Calorimetry. Analytical Biochemistry. Analytical Biochemistry. 2018; 554: 61-69. .

Schön A, Clarkson BR, Jaime M, Freire E. Temperature stability of proteins: Analysis of irreversible denaturation using isothermal calorimetry. Proteins. 2017; 85 (11): 2009-2016. doi: 10.1002/prot.25354.

Clarkson BR, Schön A, Freire E. Conformational stability and self-association equilibrium in biologics. Drug Discovery Today. 2015; 21 (2): 342-7. doi: 10.1016/j.drudis.2015.11.007.

Schön A, Clarkson BR, Siles R, Ross P, Brown RK, Freire E. Denatured state aggregation parameters derived from concentration dependence of protein stability. Analytical Biochemistry. 2015; 48:45-50. doi: 10.1016/j.ab.2015.07.013.

Eckdahl TT, Campbell AM, Heyer LJ, Poet JL, Clarkson BR…48 Undergraduate Student Coauthors. 2015. Programmed evolution for optimization of orthogonal metabolic output in bacteria. PLoS ONE. 2015;10(2):e0118322. doi:10.1371/journal.pone.0118322.

Yonemoto IT, Clarkson BR, Smith HO, Weyman PD. A broad survey reveals substitution tolerance of residues ligating FeS clusters in [NiFe] hydrogenase. BMC Biochemistry. 2014;15:10. doi:10.1186/1471-2091-15-10.

POSTER PRESENTATIONS

Benjamin R Clarkson, Rajoshi Chaudhuri, Arne Schön, Jonathan W. Cooper, Lisa Kueltzo, Ernesto Freire. “Long-Term Stability of the HIV-1 Neutralizing Monoclonal Antibody VRC07 Using Isothermal Calorimetry.” NIH Structural Biology Related to HIV/AIDS 2018. June 28-29, 2018.

Benjamin Clarkson, Arne Schön, Ernesto Freire. “Conformational stability and self-association equilibrium in formulation development for biologics.” PEGS Conference 2016, Boston, Massachusetts, April 30-May 1, 2016.

Benjamin R. Clarkson, Isaac T. Yonemoto, Philip D. Weyman. “Broad Survey Reveals Tolerance of Fe-S Clusters to Substitution in [NiFe] Hydrogenase.” Intern Poster Symposium, J. Craig Venter Institute, August 7, 2013.

Caleb Carr, David Carr, Eddie Miles, Jerrad Morton, Sachith Polpitaya, Claire Shinneman, Kamay Trueblood, Ben Clarkson, Becca Evans, Betsy Gammon, Meredith Nakano, Caroline Vrana, Laurie J. Heyer, Jeffrey L. Poet, A. Malcolm Campbell, Todd T. Eckdahl. "Developing Assembly Methods for Genetic Circuits used to Optimize Metabolic Pathways." Third Place Award, Undergraduate Student Poster Competition,

Annual Conference of the Institute for Biological Engineering, Raleigh, North Carolina, March 9, 2013.

Caroline Vrana, Ben Clarkson, Becca Evans, Betsy Gammon, Meredith Nakano, Laurie J. Heyer, A. Malcolm Campbell, Davidson College; Caleb Carr, David Carr, Eddie Miles, Jerrad Morton, Sachith Polpitaya, Kamay Trueblood, Todd T. Eckdahl, Jeffrey L. Poet, Missouri Western State University. "Using *E.coli* to Determine Optimal DNA Design for Metabolite Production." Undergraduate Student Poster Competition, Annual Conference of the Institute for Biological Engineering, Raleigh, North Carolina, March 9, 2013.